

Contributions to Mineralogy and Petrology

AMFORM, a new mass-based model for the calculation of the unit formula of amphiboles from Electron Micro-Probe analyses: calibration, recommendations and implications

--Manuscript Draft--

Manuscript Number:	
Full Title:	AMFORM, a new mass-based model for the calculation of the unit formula of amphiboles from Electron Micro-Probe analyses: calibration, recommendations and implications
Article Type:	Original Paper
Keywords:	Li-free amphiboles * unit-formula calculation * oxo component * cation mass * SREF * SIMS
Corresponding Author:	Filippo Ridolfi, PhD Leibniz Universitat Hannover Urbino, ITALY
Corresponding Author Secondary Information:	
Corresponding Author's Institution:	Leibniz Universitat Hannover
Corresponding Author's Secondary Institution:	
First Author:	Filippo Ridolfi, PhD
First Author Secondary Information:	
Order of Authors:	Filippo Ridolfi, PhD Alberto Zanetti Alberto Renzulli Diego Perugini Francois Holtz Roberta Oberti
Order of Authors Secondary Information:	
Funding Information:	
Abstract:	<p>In this work, we have studied the relationships between mass concentration and unit formula of amphibole using 114 carefully selected high-quality experimental data (EMP+SREF±SIMS analyses) of natural and synthetic Li-free monoclinic species belonging to the Ca and Na-Ca subgroups, plus Li-free and Mn-free C2/m end-members (a total of 75 ideal element oxides-formula pairs including some oxo analogues of Ca amphiboles). Theoretical considerations and regression analysis of these data allowed us to obtain a number of equations which can be used to: (i) calculate from EMP analyses a amphibole unit-formula consistent with SREF±SIMS data, (ii) discard unreliable analyses and (iii) estimate WO₂- and Fe³⁺ contents in Li-free C2/m amphiboles with relatively low Cl contents (≤0.2 atoms per formula unit). The AMFORM approach mostly relies on the fact that while the cation mass in Cl-poor amphiboles increases with the content of heavy elements, its anion mass maintains a nearly constant value, 220 + 2(OH, F, O), resulting in a very well-defined polynomial correlation between the molecular mass and the cation mass per gram (R² = 0.998). The precision in estimating the amphibole formula is 2-4 times higher than that of classic methods which follow IMA-recommended schemes. A linear relation between the WO₂- content and the sum of some C(Ti, Fe³⁺) and A(Na+K) contents, useful to estimate the iron oxidation state of highly-oxidized amphiboles typical of post-magmatic processes, is also proposed. A user-friendly spreadsheet (AMFORM.xlsx) is provided as supplementary material. This work opens new perspectives on the unit-</p>

formula calculation of other minerals containing OH and structural vacancies (e.g. micas).

[Click here to view linked References](#)

1
2
3
4 **AMFORM, a new mass-based model for the calculation of the unit formula of amphiboles from**
5
6 **Electron Micro-Probe analyses: calibration, recommendations and implications**
7
8
9

10
11
12
13 **F. Ridolfi^{1,2} · A. Zanetti³ · A. Renzulli⁴ · D. Perugini² · F. Holtz¹ · R. Oberti³**
14

15
16 ¹Institut für Mineralogie, Leibniz Universität Hannover, 30167 Hannover, Germany
17
18

19
20 ²Dipartimento di Fisica e Geologia, Università di Perugia, 06100 Perugia, Italy
21
22

23 ³CNR-Istituto di Geoscienze e Georisorse, Sede secondaria di Pavia, 27100 Pavia, Italy
24
25

26 ⁴Dipartimento di Scienze Pure e Applicate, Università degli Studi di Urbino “Carlo Bo”, 61029 Urbino,
27
28 Italy
29
30
31
32
33
34

35 **Abstract**
36
37
38

39 In this work, we have studied the relationships between mass concentration and unit formula of
40 amphibole using 114 carefully selected high-quality experimental data (EMP+SREF±SIMS analyses)
41 of natural and synthetic Li-free monoclinic species belonging to the Ca and Na-Ca subgroups, plus Li-
42 free and Mn-free *C2/m* end-members (a total of 75 ideal element oxides-formula pairs including some
43 oxo analogues of Ca amphiboles). Theoretical considerations and regression analysis of these data
44 allowed us to obtain a number of equations which can be used to: (i) calculate from EMP analyses a
45 amphibole unit-formula consistent with SREF±SIMS data, (ii) discard unreliable analyses and (iii)
46 estimate ^WO²⁻ and Fe³⁺ contents in Li-free *C2/m* amphiboles with relatively low Cl contents (≤0.2
47 atoms per formula unit). The AMFORM approach mostly relies on the fact that while the cation mass
48
49
50
51
52
53
54
55
56
57
58
59
60
61
62
63
64
65

1
2
3
4 in Cl-poor amphiboles increases with the content of heavy elements, its anion mass maintains a nearly
5
6 constant value, $22O + 2(OH, F, O)$, resulting in a very well-defined polynomial correlation between the
7
8 molecular mass and the cation mass per gram ($R^2 = 0.998$). The precision in estimating the amphibole
9
10 formula is 2-4 times higher than that of classic methods which follow IMA-recommended schemes. A
11
12 linear relation between the $^{WO^{2-}}$ content and the sum of some $^C(Ti, Fe^{3+})$ and $^A(Na+K)$ contents, useful
13
14 to estimate the iron oxidation state of highly-oxidized amphiboles typical of post-magmatic processes,
15
16 is also proposed. A user-friendly spreadsheet (AMFORM.xlsx) is provided as supplementary material.
17
18 This work opens new perspectives on the unit-formula calculation of other minerals containing OH and
19
20 structural vacancies (e.g. micas).
21
22
23
24
25

26 **Keywords**

27
28 Li-free amphiboles · unit-formula calculation · oxo component · cation mass · SREF · SIMS
29
30
31
32
33

34
35 *Corresponding author: filippo.ridolfi@uniurb.it*
36
37
38

39 **Introduction**

40
41
42
43 Amphiboles are a supergroup of silicate minerals containing, either at the major- or at the trace-element
44
45 level, most elements of geological/geochemical relevance (for a review, see Hawthorne et al. 2007). It
46
47 has been largely recognized that the role of amphibole in understanding geological/planetary processes
48
49 and several health issues is of crucial importance (e.g. Forbes and Starmer 1974; Foley et al. 2002;
50
51 Gunter et al. 2007; McCanta et al. 2008; Jackson et al. 2013; Smith 2014). Amphibole crystal-
52
53 chemistry has captured the attention of many scientists over the years because of its intrinsic
54
55 complexity (consider that even the term amphibole derives from the Greek “αμφιβολος”, which means
56
57 ambiguous; René J. Haüy 1743 – 1822; Cipriani et al. 2007), its remarkable compliance to incorporate
58
59
60
61
62
63
64
65

1
2
3
4 most elements of geological interest and ability to record the steps of a wide range of geochemical and
5
6 petrological processes due to a network of mutual relationships between cation ordering, chemistry of
7
8 the associated phases (minerals and/or melt) and intrinsic parameters such as pressure, temperature and
9
10 fugacity of volatile elements (Holland and Blundy 1994; Al'meev et al. 2002; Oberti et al. 2000,
11
12 2007a; Ridolfi et al. 2010; Ridolfi and Renzulli 2012; Zhang et al. 2017). However, the prerequisite for
13
14 using amphiboles as geological markers is the determination of their correct crystal-chemical formula
15
16 (i.e., composition and site partitioning). Routine calculations of amphibole unit-formulae from Electron
17
18 Micro-Probe (hereafter EMP) data may be seriously affected by inappropriate normalization
19
20 procedures and/or the lack of accurate information on the oxidation state of iron and the contents of
21
22 hydrogen and lithium (Leake et al. 1997; Al'meev et al. 2002; Hawthorne et al. 2012; Locock 2014).
23
24
25
26
27

28 In this work, we analyze the relation between elemental concentration (by mass) and
29
30 stoichiometry in the amphibole supergroup, and propose a new mass-based method, to be applied to the
31
32 only EMP data, that allows identification of bad analyses and calculation of the correct unit formula of
33
34 Li-free (and Mn- and Cl-poor) *C2/m* amphiboles, with an uncertainty 2-4 times lower than that of other
35
36 published procedures (Hawthorne et al. 2012; Locock 2014).
37
38
39
40
41
42
43

44 **Definitions**

45
46
47 The amphiboles are a supergroup of silicate minerals with the general formula $AB_2C_5T_8O_{22}W_2$
48
49 (Hawthorne et al. 2012). The group cations considered in this work include: A = Na, K, Ca, □
50
51 (vacancy); B = Ca, Na, Mn^{2+} , Fe^{2+} , Mg; C = Mg, Ti^{4+} , Fe^{2+} , Mn^{2+} , Cr, Ni, Zn, Al, Fe^{3+} ; T = Si, Al, Ti^{4+} ;
52
53 and W = OH^- , F, Cl, O^{2-} (where Mn, Cr, Ni, Zn and Cl are minor components, ≤ 0.2 atoms per formula
54
55 unit, apfu).
56
57
58
59
60
61
62

1
2
3
4 Below we report operative definitions useful to follow the text more easily. The sign Σ includes all
5
6 the cations and/or anions in the groups defined above; e.g. $\Sigma_A^T x$ = sum of the parameter x for all A-, B-,
7
8 C- and T-group cations, $\Sigma_A^W x$ = sum of the parameter x for A-, B-, C- and T-cations plus W-anions and
9
10
11 22 O²⁻ pfu.
12
13

- 14 - *total element oxides*: sum of cation oxides and halogens calculated excluding the measured
15
16 FeO_{tot} (total iron content) and the oxygen atoms balancing F and Cl (i.e. O^{F,Cl}), and adding
17
18 Fe₂O₃, FeO and H₂O calculated from the unit-formula, corresponding to the H₂O measured by
19
20 Secondary-Ion Mass Spectrometry (hereafter SIMS) or estimated by Single-crystal X-ray
21
22 Structure REFinement (hereafter SREF). Note that the total element oxides of EMP analyses
23
24 generally deviates from ideality (100 wt%);
25
26
- 27 - *original composition*: the concentrations expressed as wt% of the oxides (SiO₂, TiO₂, Al₂O₃,
28
29 Cr₂O₃, FeO_{tot}, NiO, ZnO, MnO, MgO, CaO, Na₂O, K₂O) and halogens (F, Cl) in the amphibole
30
31 formula, usually measured by EMP analyses;
32
33
- 34 - *normalized composition*: the concentrations expressed as wt% of the cation oxides (SiO₂, TiO₂,
35
36 etc.) and halogens (F, Cl) in amphibole calculated from the unit formula to obtain a value of the
37
38 total element oxides equal to 100 wt% (e.g. Table 1 and <http://webmineral.com> for end-
39
40 members);
41
42
- 43 - *deviated composition*: the concentrations (wt%) of the cation oxides (SiO₂, TiO₂, etc.) and
44
45 halogens (F, Cl) in amphibole forced to have a value of the total element oxides deviating from
46
47 100 wt%, specifically 98.2 and 101.8 wt%;
48
49
- 50 - *TC*: total coefficient, obtained by dividing the sum of the cation oxides (with iron as FeO_{tot}) of a
51
52 normalized composition with that of its original or deviated compositions; TC is used to modify
53
54 the original composition to obtain an adjusted composition approaching a normalized
55
56 composition (see following sections);
57
58
59
60
61

- 1
2
3
4 - M_r : molecular mass of amphibole usually calculated from its unit formula, i.e. $M_r =$
5
6 $\sum_A^W apfu \times A_r$, where A_r is the atomic mass of all elements in the formula;
7
8
9 - $cmpg$: cation mass per gram, calculated from the original, deviated or normalized compositions,
10
11 i.e. $cmpg = 10^{-2} \sum_A^T wt\%$. Note that $cmpg$ is actually a mass ratio and thus for normalized
12
13 compositions it corresponds to the total cation mass divided by the sum of the total cation and
14
15 anion masses;
16
17
18 - X_i : cation mass fraction of element i , that is the mass of element i divided by the total cation
19
20 mass (e.g. $X_{Si} = \frac{Si\ wt\%}{\sum_A^T wt\%}$, $X_F = \frac{F\ wt\%}{\sum_A^T wt\%}$); they are the same in normalized, deviated and original
21
22 compositions;
23
24
25
26 - CR : correlation ratio between the apfu and $mmol/g$ (millimole per gram) of the total cations, i.e.
27
28 $CR = \frac{\sum_A^T apfu}{\sum_A^T mmol/g}$. CR is a constant value for any normalized composition and, once precisely
29
30 determined (see below), can be easily used to calculate the apfu of each element multiplying CR
31
32 by the element concentration ($mmol/g$);
33
34
35
36 - $\Delta charge$: deviation from electroneutrality in an amphibole unit-formula (i.e. positive – negative
37
38 charge sums);
39
40
41
42 - ΔC and ΔB : deviation from 5 apfu and 2 apfu in the C- and B-group cations, respectively.
43
44
45
46
47
48
49

50 Data selection and techniques

53 Composition and petrogenesis of the investigated amphiboles

54
55 We have studied the relationships between concentration and unit formula in Li-free and Mn,Cl-poor
56
57 monoclinic amphiboles belonging to the Ca, Na-Ca subgroups (and some of their oxo analogues) based
58
59 on a dataset accurately selected in the literature and in the CNR-IGG amphibole database, according to
60
61

1
2
3
4 the presence of accurate EMP+SREF±SIMS analyses. The dataset contains 114 oxides-formula pairs
5
6 with the largest possible geochemical and geological variability; the oxo-amphiboles considered are
7
8 kaersutite, ferri-kaersutite, oxo-potassic-chromio-katophorite, oxo-potassic-taramite, Ti-rich oxo-
9
10 sadanagaite, Ti-rich oxo-pargasite and Ti-rich oxo-ferri-pargasite (see AMFORM.xlsx). Na amphibole
11
12 species were excluded because they may contain minor to moderate amounts of Li (e.g. Hawthorne et
13
14 al. 1993) which cannot be detected and measured by EMP analysis.
15
16

17
18
19 The dataset includes published oxides-formula pairs of 61 synthetic (Oberti et al. 2000; Bottazzi
20
21 et al. 1999; Tiepolo et al. 2000; 2003; Adam et al. 2007) and natural amphiboles which are typical of
22
23 geologically relevant systems (gabbro, peridotite, lherzolite, kyanite-eclogite, marble,
24
25 metasomatic/skarn-type deposit and several types of metavolcanic amphibolites) and coming from
26
27 different world-wide localities (Oberti et al. 1995; Vannucci et al. 1995; Robinson et al. 1997; Oberti et
28
29 al. 2007b; Uvarova et al. 2007; Perinelli et al. 2012; Della Ventura et al. 2014). The unpublished
30
31 oxides-formula pairs (53) come from the CNR-IGG database in Pavia and include amphiboles from
32
33 volcanic deposits, mantle ultramafic rocks (hornblendites, pyroxenites, peridotites), peridotitic and
34
35 pegmatitic veins.
36
37
38

39 40 **Characterizing methods**

41
42 All the unpublished amphiboles were analyzed by EMP, SREF and SIMS allowing a complete
43
44 characterization of their crystal-chemical parameters. SREF and SIMS analyses were done at IGG-
45
46 CNR in Pavia, while EMP analyses were mostly done at the University of Manitoba (Winnipeg,
47
48 Canada).
49
50

51
52 The crystal-chemical formulae were calculated by combining SREF, EMP and SIMS results.
53
54 The number of A cations was estimated on the basis of the refined site-scattering values at the relevant
55
56 sites and from K₂O and Na₂O contents from EMP analysis. The oxo component was evaluated either
57
58 by SIMS or by a SIMS-calibrated crystal-chemical relationship (Oberti et al. 2007a), so that the Fe³⁺
59
60

1
2
3
4 content can be derived based on the overall electroneutrality. The Fe^{3+} content and its distribution were
5
6 further constrained through the pattern of refined mean bond-lengths observed at the three $M(1-3)$
7
8 octahedra. The presence of the $M(4')$ subsite, indicating the occurrence of small B cations (Mn^{2+} , Fe^{2+} ,
9
10 Mg), was checked on the difference Fourier maps. B cations were calculated assigning excess C cations
11
12 (first Mn^{2+} and then Fe^{2+} and Mg) to minimize the difference between the site scattering calculated
13
14 (from EMP) for the B and C cations and those obtained by SREF. As a further check, the $^{\text{T}}\text{Al}$ contents
15
16 obtained by recalculation of EMP analyses are in close agreement with those calculated from the
17
18 refined $\langle T(1)\text{-O} \rangle$ and $\langle T(2)\text{-O} \rangle$ distances (Oberti et al. 2007a).
19
20
21
22

23
24 Many of the amphiboles taken from the literature include EMP, SREF and SIMS data, and their
25
26 formulae were obtained following the same procedure. The amphibole formula selected from the article
27
28 of Robinson et al. (1997) was derived from EMP, SREF, Mössbauer (for $\text{Fe}^{3+}/\text{Fe}_{\text{tot}}$), wet-chemical (for
29
30 F) and IR (InfraRed spectroscopy, for H_2O) analyses. In some cases, the formulae were derived from
31
32 EMP and SREF data only (Oberti et al. 1995; Vannucci et al. 1995; Oberti et al. 2007b; Della Ventura
33
34 et al. 2014), and the oxo component was estimated using a correlation developed at CNR-IGG in Pavia
35
36 based on SREF results (Oberti et al. 2007a). In other cases, the Fe^{3+} content of the amphibole was
37
38 validated by Mössbauer spectroscopy (Uvarova et al. 2007, Perinelli et al. 2012). The amphibole data
39
40 selected from the older article (Oberti et al. 1995) the occurrence of $^{\text{w}}\text{O}^{2-}$ in amphibole was estimated
41
42 during this work using the published SREF data (see above).
43
44
45
46
47

48 **Selection criteria of the calibration data**

49
50 Both literature and unpublished amphiboles were processed using a series of criteria to guarantee as
51
52 much as possible the selection of a calibration dataset characterized by high-quality data.
53
54

55 We first discarded amphibole compositions showing standard deviations (σ) of the EMP
56
57 element oxides higher than $2/3$ of the average oxide σ values for the experimental amphiboles reported
58
59 in Table 2 of Ridolfi and Renzulli (2012). We discarded also the amphibole compositions with total
60
61

1
2
3
4 element oxides falling outside the range of 100 ± 1.7 wt%, because large deviations from 100 wt% may
5
6 derive from analytical problems for some elements, resulting in error propagation to the unit formula.
7
8 The amphibole compositions in the dataset have total element oxides ranging from 98.3 to 100.8 wt%
9
10 although most of the totals are lower than 100 wt%, with an average value of 99.3 wt%.

11
12
13
14 Amphibole formulae showing $\Delta charge$ larger than ± 0.05 , ΔC and ΔB larger than ± 0.01 and/or
15
16 total cations higher than 16.005 apfu were also discarded. In addition, formulae calculated without
17
18 considering the oxo component, i.e. forcing the negative charges to be 46, were not considered. The
19
20 bijection between the composition and formula of any amphibole was carefully checked comparing the
21
22 CR values for each major cations (e.g. $CR^{Si} = \frac{Si\ apfu}{Si\ mmol/g}$) with the CR calculated on the total cation sum
23
24 (as defined above). This procedure allowed us to avoid mismatches between formulae and
25
26 compositions due to adjustment and/or editing.
27
28
29
30

31
32 This final database contains 114 entries and is included in the AMFORM.xlsx spreadsheet
33
34 (provided as supplementary material). The ranges in elemental composition are: Si = 5.8-7.8 apfu;
35
36 $\sum(Ca+Na+K) = 0.1-1.0$ apfu; F \leq 1.3 apfu; Cl \leq 0.2 apfu; Mg/(Mg+Fe²⁺) = 0.2-1.0; Fe³⁺/Fe_{tot} = 0.0-1.0.
37
38

39 It is worth noting that oxides-formula pairs not validated by SREF were not included in the final
40
41 dataset. This decision was taken to guarantee an independent check of the formulae and a reliable
42
43 constraint on the total number of cations.
44

45
46 Beside the 114 selected amphibole compositions, we used ideal formulae and compositions of
47
48 selected Li- and Mn-free *C2/m* end-members of the amphibole supergroup (Hawthorne et al. 2012)
49
50 (Table 1). The 75 oxides-formula pairs in Table 1 also include kaersutite, ferri-kaersutite, ferro-
51
52 kaersutite, ferro-ferri-kaersutite and some oxo analogues of the Ca groups as these amphiboles in
53
54 nature may often have a significant oxo-component.
55
56
57
58
59
60
61
62
63
64
65

Rationale and data analyses

The high-quality dataset described above was used to analyze any possible relation between compositional (e.g. wt% and *mmol/g*) and unit-formula parameters in amphiboles.

For a complete characterization of the amphibole unit-formula, two crucial parameters must be determined: the total cation content (ranging from 15 to 16 apfu) and the oxo component ($^{\text{W}}\text{O}^{2-}$), which allows the sum of the negative charges to vary between 46 and 48. When these parameters are known and the presence of Mn^{3+} can be excluded, the amount of Fe^{3+} can be obtained under the constraint of electroneutrality.

Development of the CR-equations

The correlation ratio (*CR*) between apfu and *mmol/g* of any component or sum of components (e.g. Si, total aluminium Al_{T} , F, total cations) must be constant for any normalized and end-member composition-formula pair. If *CR* is known with a reasonably good approximation, the apfu content of each element can be calculated multiplying *CR* by its concentration in *mmol/g*.

Figure 1a shows that the *CR* of the normalized and end-member compositions is perfectly correlated with their molecular mass, M_r :

$$CR = 10^{-3}M_r \quad (R^2 = 1.000) \quad (1)$$

The original compositions only slightly deviate from this linear trend. The deviations is due to the total element oxides which are usually are lower than 100% (see above). In Figure 1a, the end-member sample with the lowest M_r is cummingtonite, $\square\text{Mg}_2\text{Mg}_5\text{Si}_8\text{O}_{22}(\text{OH})_2$, and that with the highest M_r is ferro-ferri-cannilloite, $\text{CaCa}_2(\text{Fe}^{2+}_4\text{Fe}^{3+})(\text{Si}_5\text{Al}_3)\text{O}_{22}(\text{OH})_2$.

Note that equation 1 is valid for any type of mineral or compound, and should be used at the end of any formula calculation procedure to validate the final results and the quality of the data (see

1
2
3
4 below). However, this simple correlation cannot be used to estimate CR from EMP analysis because M_r
5
6 can only be calculated from the formula.
7
8

9 Figure 1b shows that the CR values of normalized and end-member compositions have a nearly
10 perfect polynomial relation with the cation mass per gram, $cmpg$, which can be directly calculated from
11 EMP data (see above):
12
13

$$14 \quad CR = 4.809cmpg^2 - 3.409cmpg + 1.276 \quad (R^2 = 0.998) \quad (2)$$

15
16 Indeed, the anion components in the different amphibole compositions have almost the same
17 mass, because they mostly consist of the same number of ions with similar A_r , $22O^{2-} + 2(OH^-, F^-, O^{2-})$.
18
19 In contrast, the mass of the cation component increases with the amount of heavier cations (e.g. Fe^{2+} ,
20 Fe^{3+}) resulting in a progressively increasing pattern of CR (and M_r) with $cmpg$. Because $cmpg$ is a mass
21 ratio, Figure 1b has a curvilinear trend, in agreement with the general rules for correlations in mixing
22 binary systems (Langmuir et al. 1978). The small scattering observed for some normalized and end-
23 member compositions ($R^2 = 0.998$; Fig. 1b) is due to the occurrence of $^W(Cl^-, F^-, O^{2-})$, which have A_r
24 different from that of OH^- , thus affecting the $cmpg$ values. For example, the heaviest end-member
25 ferro-ferri-cannilloite has the same cation mass of its oxo analogue but a higher M_r value because it
26 differs (in mass term) by having two more hydrogen atoms (Table 1). Therefore, the mass of W anions
27 is higher than that of its oxo equivalent (because OH^- is heavier than O^{2-}) resulting in a $cmpg$ value
28 slightly lower than that of oxo ferro-ferri-cannilloite (Fig. 1b; Table 1). F-rich amphiboles behave in
29 the opposite way because F^- has a mass higher than OH^- . However the effect of $^WF^-$ and $^WO^{2-}$ in
30 calculating CR is minimal as confirmed by the high determination coefficient (R^2) of equation 2 (Fig.
31 1b), so that amphibole compositions with high F and oxo contents can be treated with this method with
32 a sufficient accuracy.
33
34
35
36
37
38
39
40
41
42
43
44
45
46
47
48
49
50
51
52
53
54
55
56

57 In contrast, amphiboles with high Cl contents (e.g. Ridolfi et al. 2010) deviate significantly
58 from equation 2 (towards lower $cmpg$) because the A_r of chlorine is about twice that of F, OH and O.
59
60
61

1
2
3
4 However, the maximum Cl content in the high-quality analyses of amphiboles is 0.20 apfu
5
6 (corresponding to 0.72 wt%) and does not produce large deviations from equation 2. This is because
7
8 the incorporation of Cl in amphibole is related to high Fe²⁺ contents (e.g. Oberti et al. 2007a) which
9
10 results in relatively low *cmpg* underestimations (e.g. in the two Fe- and Cl-rich amphiboles marked
11
12 with green triangles in Fig. 1b).
13
14

15
16 It is worth noting that equation 2 cannot be successfully applied to the original compositions of
17
18 most of the amphiboles because EMP uncertainties commonly result in incorrect *CR* and *cmpg* values
19
20 leading to significant deviations from the normalized composition, i.e. from total element oxides equal
21
22 to 100 wt% (Fig. 1). Therefore, at least a preliminary estimation of ^WO²⁻ and H₂O is required. This
23
24 issue is discussed in more detail in the section “Total coefficient and calculation procedure”.
25
26

27 28 **The oxo component, ^WO²⁻**

29
30
31 It is commonly accepted that ^WO²⁻ and ^WOH⁻ contents in amphibole mostly depend on two substitution
32
33 mechanisms involving cations occurring at the *M*(1) and *M*(3) sites:
34
35



38
39
40
41 During igneous and metamorphic processes, the OH⁻ content of amphibole is mostly ruled by
42
43 substitution mechanism (a) wherein the amount of OH⁻ at the W site is reduced by twice the amount of
44
45 Ti incorporated at the *M*(1) site. Substitution (a) mostly occurs at high-T low-*f*H₂O conditions, and
46
47 involves chemical exchange of major components such as Mg, Fe²⁺ and Ti with the surrounding
48
49 environment (glass, minerals). During magma ascent or hydrothermal alteration, amphibole may
50
51 undergo a high T-*f*O₂ process of deprotonation involving iron oxidation according to substitution
52
53 mechanism (b) (e.g. King et al. 1999; Oberti et al. 2007a, Popp et al. 2006).
54
55
56

57
58 From a crystal-chemical viewpoint, the occurrence of ^WO²⁻ implies important changes in the
59
60 cation-ordering scheme typical of amphiboles, where high-charged C cations fully ordered at the *M*(2)
61
62

1
2
3
4 site, with the only exception of Al, which may disorder between the $M(2)$ and $M(3)$ sites in high-T Mg-
5 rich pargasites and edenites (Oberti et al 1995; Della Ventura et al 2014). The different bond-valence
6 bond-strength requirements of the O(3) oxygen after H^+ loss must be satisfied by the presence of high-
7 charged cations at the coordinated $M(1)$ (with multiplicity 2) and $M(3)$ sites. This feature implies
8 complex but strongly related compositional changes in the amphibole solid-solution system, that can be
9 empirically approached using multivariate least-square analysis (Ridolfi and Renzulli 2012; Ridolfi et
10 al. 2014; Zhang et al. 2017).

11
12
13
14
15
16
17
18
19
20
21 Among the 114 amphiboles in the dataset, 87 formulae have ${}^W O^{2-} \leq 2$ ${}^C Ti$ implying that
22 mechanism (b) is almost not active. Hereafter, for these amphiboles we will use the prefix “poorly-
23 oxidized” to remind that the amount of ${}^{M(1,3)} Fe^{3+}$ due to post-crystallization oxidation is zero or very
24 low. These amphiboles may contain up to 1.3 apfu ${}^W O^{2-}$, which mostly derives from the substitution
25 mechanism (a). However, the use of total Ti in C (${}^C Ti$) as a proxy for the oxo component (Hawthorne et
26 al. 2012; Locock 2014) may be severely misleading because in these samples a significant amount of
27 ${}^C Ti$ is often ordered at the $M(2)$ site and hence does not contribute to reaction (a) (Oberti et al. 2007a).

28
29
30
31
32
33
34
35
36
37
38 Regression analysis shows that the ${}^W O^{2-}$ content in poorly-oxidized amphiboles (with ${}^W O^{2-} \leq$
39 $2{}^C Ti$) can be estimated with reasonably low errors (Fig. 2a) using the following equation:

$$\begin{aligned}
 {}^W O^{2-} = & -6.684X_{Si} + 11.025X_{Ti} - 0.989X_{Al} - 2.800X_{Fe} - 20.359X_{Mn} - 0.903X_{Mg} - 6.875X_{Ca} - \\
 & 11.119X_{Na} - 2.553X_K + 5.751X_F + 4.610 \text{ (apfu)} \quad (3)
 \end{aligned}$$

40
41
42
43
44
45
46
47
48 This equation can be applied without any previous calculation of the amphibole formula, as it only
49 depends on the values of cation fraction (X_i) calculated from EMP analyses. In addition, the X_i values
50 are the same in both original and normalized compositions because generalized
51 overestimation/underestimation does not change the mass ratios (see above). The statistic error σ_{est}
52 (standard error of estimate) for poorly-oxidized amphiboles (0.10 apfu; Fig. 2a) is comparable to SIMS
53
54
55
56
57
58
59
60
61
62
63
64
65

1
2
3
4 uncertainty in hydrogen measurement ($\pm 10\%$ relative; e.g. Oberti et al. 2007a) supporting the validity
5
6 of equation 3.
7

8
9 A drawback of equation 3 is that it underestimates ${}^W\text{O}^{2-}$ in highly-oxidized amphiboles (where
10
11 ${}^W\text{O}^{2-} > 2^{\text{C}}\text{Ti}$), which underwent high-T, high- $f\text{O}_2$ post-magmatic and/or hydrothermal alteration
12
13 according to mechanism (b). However, this issue may even turn out to be an advantage when studying
14
15 the processes of amphibole magmatic crystallization (e.g. Ridolfi et al. 2010; Ridolfi and Renzulli
16
17 2012; Ridolfi et al. 2016; Zhang et al. 2017). In fact, the higher value of $f\text{O}_2$ in high-T magmatic
18
19 environments ($\sim 10^{-7}$ bar, corresponding to a $\log f\text{O}_2$ of 3-4 units above the Ni-NiO buffer; Ridolfi and
20
21 Renzulli 2012) is several orders of magnitude lower than in air (~ 0.21 bar, i.e. $-0.68 \log f\text{O}_2$; Namur et
22
23 al. 2012) where high-T post-magmatic oxidation most probably occurs. It is worth noting that the
24
25 highly-oxidized amphiboles in our database are Ca-dominant megacrysts (rapidly ejected to the surface
26
27 from high T-P conditions) or mantle amphiboles which underwent hydrothermal alteration.
28
29
30
31
32

33
34 At this point, we looked for correlations between the measured values of ${}^W\text{O}^{2-}$ and cation
35
36 compositional parameters in both poorly and highly oxidized amphiboles, starting from the observation
37
38 that the fractions of Ti and Fe^{3+} occurring at the $M(1)$ and $M(3)$ sites are directly involved in the
39
40 process of deprotonation. The best correlation we found is reported in Figure 2b for the 114
41
42 amphiboles in the dataset, i.e. ${}^W\text{O}^{2-} = 0.963[4/3^{\text{C}}\text{Ti} + 2/3^{\text{C}}\text{Fe}^{3+} + 2/3^{\text{A}}(\text{Na}+\text{K})] - 0.624$. The overall
43
44 correlation shows a reasonably good R^2 value (0.927) and closely approaches the equation:
45
46
47

$${}^W\text{O}^{2-} = 4/3^{\text{C}}\text{Ti} + 2/3^{\text{C}}\text{Fe}^{3+} + 2/3^{\text{A}}(\text{Na}+\text{K}) - 2/3 \text{ apfu} \quad (4a)$$

48
49

50
51 Equation 4a works well for both poorly (${}^W\text{O}^{2-} \leq 2^{\text{C}}\text{Ti}$) and highly (${}^W\text{O}^{2-} > 2^{\text{C}}\text{Ti}$) oxidized amphiboles
52
53 when $4/3^{\text{C}}\text{Ti} + 2/3^{\text{C}}\text{Fe}^{3+} + 2/3^{\text{A}}(\text{Na}+\text{K})$ is $\geq 2/3$. In that region, the only two samples significantly
54
55 deviating from equation 4a (${}^W\text{O}^{2-}$ overestimation up to 0.49 apfu) are rare and peculiar Na-Ca
56
57 amphiboles, i.e. alumino-taramite K22-2 and fluoro-alumino-magnesio-taramite DJ102-23, which are
58
59
60
61
62

1
2
3
4 characterized by high ${}^{\text{C}}\text{Fe}^{3+}$ and A-cations contents but, according to their crystal-chemical
5
6 characterization do not contain oxo component (Oberti et al. 2007b; Fig. 2b).
7
8

9 In Figure 2b, amphibole compositions with $4/3{}^{\text{C}}\text{Ti} + 2/3{}^{\text{C}}\text{Fe}^{3+} + 2/3{}^{\text{A}}(\text{Na}+\text{K}) \leq 2/3$ have zero or
10
11 negligible ${}^{\text{W}}\text{O}^{2-}$ contents, providing the constraint:
12
13

$$14 \quad {}^{\text{W}}\text{O}^{2-} = 0 \text{ apfu when } 4/3{}^{\text{C}}\text{Ti} + 2/3{}^{\text{C}}\text{Fe}^{3+} + 2/3{}^{\text{A}}(\text{Na}+\text{K}) \leq 2/3 \text{ apfu} \quad (4b)$$

15
16 When applying equations 4a and constraint 4b we obtain a $\sigma_{\text{est}} = 0.12$ apfu in the whole dataset (Fig.
17
18 2b). This error is also consistent with the error in H measurements by SIMS ($\pm 10\%$ relative), thus
19
20 supporting the validity of our approach. When the two major outliers alumino-taramite K22-2 and
21
22 fluoro-alumino-magnesio-taramite DJ102-23 are not considered, the maximum error decreases from
23
24 0.49 to 0.3 apfu which is even lower than that indicated by equation 3 for the only poorly-oxidized
25
26 amphiboles (0.4 apfu; Fig. 2a).
27
28
29
30

31 Equation (4a) and constraint (4b) can be easily applied to any amphibole unit-formula anytime
32
33 an independent measurement of $\text{Fe}^{3+}/\text{Fe}_{\text{tot}}$ is available. When this is not the case, ${}^{\text{W}}\text{O}^{2-}$ and Fe^{3+}
34
35 contents can be estimated using a system of two linear equations including (4a) and the charge balance
36
37 equation:
38
39

$$40 \quad 4(\text{Si}+\text{Ti}) + 3(\text{Al}+\text{Cr}+\text{Fe}^{3+}) + 2[\text{Mg}+(\text{Fe}_{\text{tot}}-\text{Fe}^{3+})+\text{Mn}+\text{Ni}+\text{Zn}+\text{Ca}] + \text{Na}+\text{K} = 46 + {}^{\text{W}}\text{O}^{2-} \quad (4c)$$

41
42 where the uncertainty of the ${}^{\text{W}}\text{O}^{2-}$ and Fe^{3+} estimates depends on the errors of cation estimation
43
44 multiplied by their ionic charge.
45
46
47

48 The presence of the A cations in equations 4a,b may be explained by their capability to help in
49
50 the local electroneutrality around the O(3) site, where deprotonation occur. Recent *in operando* studies
51
52 combining SREF and FTIR (Fourier Transform Infrared Spectroscopy) showed that deprotonation
53
54 preferentially occurs close to an occupied A site, so that deprotonation is faster in amphibole
55
56 compositions with fully occupied A sites (Susta et al. 2016; Della Ventura et al. 2017 and work in
57
58 progress).
59
60
61

Total coefficient and calculation procedure

In the previous section, we have stressed that the application of equation 2 is biased by the errors of EMP analysis (Fig. 1). In order to overcome this problem, we first used equations 2 and 3 to calculate a preliminary formula for the high-quality amphibole data imposing total element oxides of 100 (normalized compositions), 98.2 and 101.8 wt% (deviated compositions). The resulting TC values are 1 for normalized compositions, < 1 for overestimated compositions and > 1 for underestimated compositions. Fe_2O_3 and FeO concentrations, $O^{F,Cl}$, and $\Delta charge$ can also be calculated from these preliminary unit formula. Multivariate least-square analysis on these 342 (114 x 3) data provided the following equation to be used to calculate total coefficient (TC):

$$TC = -7.9 * 10^{-4}SiO_2 + 6 * 10^{-4}TiO_2 - 6.6 * 10^{-4}Al_2O_3 + 8.75 * 10^{-5}Fe_2O_3 - 9.4 * 10^{-4}FeO - 8.5 * 10^{-4}MgO - 1.1 * 10^{-3}CaO - 1.48 * 10^{-3}Na_2O - 8.6 * 10^{-4}K_2O - 9.62 * 10^{-3}O^{F,Cl} + 6.41 * 10^{-3}H_2O - 9.57 * 10^{-3}Total\ element\ oxides + 4.13 * 10^{-4}\Delta charge + 2.024 \quad (5)$$

where SiO_2 to K_2O are original or deviated element oxides (wt%). The calculate regression parameters are $R^2 = 0.992$ and $\sigma_{est} = 0.001$.

If the TC values are applied to the original wt% concentrations, the resulting adjusted compositions closely approach the normalized wt% concentrations of the element oxides. These adjusted compositions can then be used to obtain amphibole formulae using again equations (2) and (3). This second stage of calculations for the 114 amphiboles in our high-quality dataset produces a statistic error (σ_{est}) for the total cation sum of 0.055 apfu. The resulting formulae can be adjusted further using a series of constrains valid for Li-free and Mn-poor amphiboles (Hawthorne et al. 2012) as follows:

- i) $Si \leq 8$ apfu;

- 1
2
3
4 ii) $\text{Si} + \text{Al} + \text{Ti} \geq 8 \text{ apfu}$;
5
6 iii) $(\text{Si} + \text{Ti} + \text{Al} + \text{Cr} + \text{Fe}_{\text{tot}} + \text{Mn} + \text{Ni} + \text{Zn} + \text{Mg}) \geq 13 \text{ apfu}$;
7
8
9 iv) $15 \leq \text{total cations (i.e. } \sum_A^T \text{ apfu)} \leq 16$;
10
11 v) $46 + {}^{\text{W}}\text{O}^{2-} \geq \text{charges due to all the cations, with Fe}_{\text{tot}}$ (total iron) charge equal to 2^+ .
12
13

14 When applying the constraints reported above to the apfu calculated from the high-quality
15 amphibole compositions, only sporadic and very minor adjustments involving constraint (iv) are
16 observed (a few calculated formulae indicate total cations slightly higher than 16). In the dataset, the
17 re-calculated total element oxides span from 99.6 to 100.5 wt%, and the final σ_{est} values for the total
18 cations and Si contents are 0.042 and 0.017 apfu, respectively. The amount of Fe^{3+} (and Fe^{2+}) can then
19 be calculated by charge balance (eq. 4c). The ${}^{\text{W}}\text{O}^{2-}$, Fe^{3+} and Fe^{2+} contents can be independently
20 estimated using the system of two linear equations (i.e. 4a and 4c):
21
22
23
24
25
26
27
28
29

30
31 - ${}^{\text{W}}\text{O}^{2-} = 4/3^{\text{C}}\text{Ti} + 2/3\text{Fe}^{3+} + 2/3^{\text{A}}(\text{Na}+\text{K}) - 2/3$
32
33 - $4(\text{Si}+\text{Ti}) + 3(\text{Al}+\text{Cr}+\text{Fe}^{3+}) + 2(\text{Mg}+\text{Fe}_{\text{tot}}-\text{Fe}^{3+}+\text{Mn}+\text{Ni}+\text{Zn}+\text{Ca}) + \text{Na}+\text{K} = 46 + {}^{\text{W}}\text{O}^{2-}$
34
35
36

37 The condition expressed in the constraint 4b should be respected and the priority in adjusting ${}^{\text{W}}\text{O}^{2-}$
38 and Fe^{3+} values should be given to charge balance (i.e. eq. 4c) considering that Δcharge can be as high
39 as 0.1 due to error propagation in the solutions of this system.
40
41
42
43

44 The final formulae are used to calculate the molecular mass, $M_r^F (\sum_A^W \text{ apfu} \times A_r)$. M_r^F should
45 closely approach the molecular mass calculated with equation 1 (i.e. $M_r^{\text{CR}} = 10^3 \text{ CR}$) using the CR
46 value obtained after the application of equation 1 to the adjusted compositions (see above). In our
47 database, deviation percentages among these molecular masses ($\Delta\text{MM}\% = 200 \frac{M_r^F - M_r^{\text{CR}}}{M_r^F + M_r^{\text{CR}}}$) range
48 between -0.60 and 0.74%.
49
50
51
52
53
54
55
56

57 A step by step procedure to calculate amphibole unit-formulae is reported in a flowchart attached to
58 this article as supplementary material. The whole procedure is included in a user-friendly Excel
59
60
61
62
63
64
65

1
2
3
4 spreadsheet (also provided as supplementary material) called AMFORM. By default, this spreadsheet
5
6 gives the ${}^{\text{W}}\text{O}^{2-}$ and Fe^{3+} values calculated according to equations 3 and 4c, but it also allows the use of
7
8 the optional method (eq. 4a-c). We strongly recommend the use of this spreadsheet to avoid errors due
9
10 to typing or unavoidable approximations of the coefficients reported in this article.
11
12

13
14 AMFORM also provides warnings for bad analyses and deviations from the correct stoichiometry
15
16 such as recalculated initial totals < 98.2 and > 101.8 wt%, sum of C and B cations < 5 and 2 apfu,
17
18 respectively (i.e. negative ΔC and ΔB) and $\Delta\text{MM}\% < -0.60$ and $> 0.74\%$.
19
20
21
22
23

24 **Testing the AMFORM approach**

25
26
27 To allow for an independent validation of the AMFORM approach, a test was made using additional 41
28
29 amphibole compositions belonging to the Ca, Na-Ca, Na and oxo groups, taken from the literature
30
31 (King et al. 2000; Tiepolo et al. 2001; Oberti et al. 2000, 2003, 2010, 2015, 2016, 2017; Uvarova et al.
32
33 2007; Satoh et al. 2004; Della Ventura et al. 2014; Gentili et al. 2015; Gatta et al. 2017) or still
34
35 unpublished (CNR-Pavia), which have been analyzed with EMP \pm SREF \pm SIMS and other techniques for
36
37 $\text{Fe}^{3+}/\text{Fe}_{\text{tot}}$ measurements (see above). It is worth noting that these amphiboles generally have higher
38
39 uncertainties (e.g. total element oxides of 97-102 wt%; ΔC from -0.07 to 0.01 apfu; Δcharge from -0.09
40
41 to 0.07) than those selected for the calibration of the AMFORM procedure (see the attached AMFORM
42
43 spreadsheet for these test lower-quality data).
44
45
46
47
48
49

50 Table 2 and Figure 4 compare the capability of AMFORM to estimate the cation and anion
51
52 contents in both high-quality (calibration, blue diamonds) and lower-quality (test, yellow triangles)
53
54 analyses. The generally higher $\Delta\text{MM}\%$ values of the test data suggest that this parameter is useful in
55
56 warning of large analytical EMP errors (Table 2). The reliability of AMFORM is further confirmed by
57
58 the homogeneous distribution around the 1:1 line of the lower-quality analyses and the absence of
59
60
61
62
63
64
65

1
2
3
4 outliers (Fig. 4). The few Li-free Na amphibole used to test AMFORM suggest that the method is
5
6 reliable also in the case of Na amphiboles (e.g. Fig. 4c), for which the calibration is based solely on
7
8 end-member compositions (Table 1; Fig. 1b).
9

10 **A comparison between the AMFORM and the Locock (2014) spreadsheets**

11
12
13
14
15 The parameters most difficult to quantify in the calculation of the amphibole unit-formula are the ^CAl
16
17 and the $^C\text{Fe}^{3+}$ contents and the number of A cations, $^A(\text{Ca} + \text{Na} + \text{K})$ (e.g. Leake et al. 1997; Al'meev et
18
19 al. 2002; Ridolfi et al. 2010). In Figure 5, we compare the results obtained for these parameters with
20
21 AMFORM to those calculated by the spreadsheet proposed by Locock (2014), which is based on the
22
23 procedures suggested in the IMA 2012 classification scheme (Hawthorne et al. 2012). When the
24
25 $\text{Fe}^{3+}/\text{Fe}_{\text{tot}}$ ratio, and/or the H_2O and Li contents are unknown (i.e., when only EMP analyses are
26
27 available), the Locock (2014) spreadsheet provides two automatic procedures, depending on the
28
29 presence or absence of $^W\text{O}^{2-}$. The Fe^{3+} contents resulting from AMFORM are those of the default $^W\text{O}^{2-}$
30
31 method (eq. 3 and 4c).
32
33
34
35

36
37 Considering the unit formulae of the high-quality amphibole compositions as reference data (i.e.
38
39 cation contents that for their high-quality better approach the effective unit formulae), the errors of the
40
41 AMFORM procedure are, on average, 2 to 4 times lower than those obtained with the spreadsheet
42
43 proposed by Locock (2014) (Fig. 5).
44
45

46
47 Locock (2014) tends to underestimate ^CAl and $^A(\text{Ca} + \text{Na} + \text{K})$ in reference amphiboles with
48
49 total cation contents close to 16 apfu, and slightly overestimates the same parameters when the total
50
51 cation content is close to 15 apfu. Concerning the estimation of the Fe^{3+} content, Locock (2014)
52
53 methods with and without $^W\text{O}^{2-}$ estimates, behaves similarly to the 13- and 15-cations methods by
54
55 IMA-1997 (Leake et al. 1997) as they generally produce either large overestimations and or large
56
57 underestimations, respectively (Fig. 5).
58
59
60
61
62
63
64
65

1
2
3
4 For an independent validation of the AMFORM approach, we tested a subset of 13 published
5
6 compositions of poorly-oxidized amphiboles for which Fe^{3+} had been measured by Synchrotron X-ray
7
8 Fluorescence (SXRF; King et al. 2000), KMnO_4 titration (Satoh et al. 2004) or X-ray Absorption Near
9
10 Edge Structure (XANES) spectroscopy (Bonadiman et al. 2014). These data had not been included in
11
12 our high-quality dataset either because they had not been examined by SREF or because they had high
13
14 Δcharge values (up to ± 0.13 ; see the attached AMFORM spreadsheet for these test data). When their
15
16 reference Fe^{3+} values are compared to those obtained by AMFORM (yellow squares in Fig. 5c), they
17
18 approach the 1:1 line and have deviations (from -0.14 to +0.16 apfu) well within the maximum-
19
20 minimum error range of the AMFORM procedure.
21
22
23
24

25 26 **An evaluation of the two methods used by AMFORM to calculate WO^{2-} and Fe^{3+}**

27
28
29 Figure 6 reports plots and statistics obtained by using the default (eq. 3, 4c) and the optional (eq. 4a-c)
30
31 methods to calculate the WO^{2-} and Fe^{3+} contents for 127 amphibole compositions (the 114 high-quality
32
33 compositions used for calibration and the 13 lower-quality compositions where $\text{Fe}^{3+}/\text{Fe}_{\text{tot}}$ values were
34
35 measured as discussed in the previous paragraph and in Figure 5c).
36
37
38

39 The default method in AMFORM is particularly useful to estimate the amount of WO^{2-} and Fe^{3+}
40
41 in poorly-oxidized amphiboles, those in equilibrium with the melt and/or other minerals. Indeed, these
42
43 amphiboles are very close to (and distributed homogeneously around) the 1:1 line in Figures 6a,b and
44
45 their WO^{2-} and Fe^{3+} contents can be estimated with a reasonably low uncertainty (± 0.1 apfu; see Figs.
46
47 2a and 4c). In contrast, in the case of highly-oxidized amphiboles, i.e. those which underwent
48
49 hydrothermal and post-crystallization oxidation, the default method may provide significant
50
51 underestimation (up to 1.2 apfu, $\sigma_{\text{est}} = 0.5$ apfu; Fig. 6a,b) and therefore cannot be used to study
52
53 metasomatic and oxidation processes during magma ascent (Dyar et al. 1993; King et al. 1999; Popp et
54
55 al. 2006; Oberti et al. 2007a). Hence, we suggest to use the optional method for these amphiboles,
56
57 because it provides a roughly homogeneous distribution around the 1:1 line in the plots in Figures 6c,d.
58
59
60
61
62
63
64
65

1
2
3
4 The larger uncertainties in estimating ${}^W\text{O}^{2-}$ and Fe^{3+} values (up to 1.2 apfu, $\sigma_{\text{est}} = 0.3$ apfu) by this
5
6 method are due to the large and unavoidable error propagation in the system of two linear equations
7
8 (eq. 4a and 4c) and variables (${}^W\text{O}^{2-}$ and Fe^{3+}).
9
10

11 12 13 14 **Final remarks and recommendations**

15
16
17 Figures 4 and Table 2 demonstrate the ability of the AMFORM approach to quantify, based solely on
18
19 EMP data, the most critical parameters in the unit formula of amphiboles with a satisfactory reliability.
20
21 It is worth noting that the proposed approach has been calibrated and is consistent with crystal-
22
23 chemical formulae obtained by combining high-quality structure refinement and analytical data.
24
25

26
27 The AMFORM procedure has been calibrated and validated for petrologically-relevant *C2/m*
28
29 amphibole compositions (oxo, Ca, Na-Ca, and Na amphiboles, considering only Li- and Mn-free end-
30
31 member compositions). The presence of significant Li and Cl contents would strongly affect the results
32
33 because their lower cation mass and higher anion mass, respectively, can largely affect the behavior of
34
35 the *CR-cmpg* relationship. Indeed, AMFORM should be applied only to amphiboles with Cl < 0.2 apfu
36
37 (~1 wt%), Also, AMFORM only accounts for Mn^{2+} and hence cannot be used to constrain the formula
38
39 of Mn^{3+} -rich amphiboles (e.g. dellaventuraite, ungarrettiite; e.g. Hawthorne et al. 1995; Hawthorne et al.
40
41 2012).
42
43
44

45
46 However, AMFORM automatically provides warnings anytime the composition proposed
47
48 deviates too much from the calibration dataset and the calculated total element oxides (both initial and
49
50 adjusted) deviate too much from those of the calibration amphiboles.
51
52

53
54 The default procedure to estimate ${}^W\text{O}^{2-}$ and Fe^{3+} contents is particularly recommended for
55
56 stability and thermobarometric studies aiming at constraining the magma pre-eruptive conditions and
57
58 storage from the amphibole composition of volcanic rocks. For this purpose, the inability of estimating
59
60
61

1
2
3
4 the Fe³⁺ content related to hydrothermal or post-magmatic oxidizing processes may even be considered
5
6 as an advantage (Ridolfi et al. 2010; Ridolfi and Renzulli 2012; Ridolfi et al. 2016). In any case, this
7
8 Fe³⁺ component can be roughly estimated using the optional ^WO²⁻ and Fe³⁺ results in AMFORM.xlsx.
9
10

11 The mass-based method proposed in this work may open a new perspective in the calculation of
12
13 the unit formula of other minerals, and is particularly useful for OH-bearing phases characterized by
14
15 structural vacancies, where the total number of cation is not known. While equation 1 is valid for any
16
17 type of chemical compound and mineral, equation 2 must be adapted to other phases with different
18
19 proportions of anion and cation sites in order to allow a reliable estimate of *CR*, and thus, of the total
20
21 cation contents.
22
23
24
25
26
27
28

29 **Acknowledgments**

30
31
32 This work was supported by a fellowship of the Alexander Von Humboldt Foundation awarded to the
33
34 first author in June 2016. We are finally grateful to R.R. Al'meev and O. Namur (Leibniz Universität
35
36 Hannover) for their critical readings of the manuscript.
37
38
39
40
41

42 **References**

- 43
44
45 Adam J, Oberti R, Cámara F, Green TH (2007) An electron microprobe, LAM-ICP-MS and single-
46
47 crystal X-ray structure refinement study of the effect of pressure, melt-H₂O concentration and
48
49 fO₂ on experimentally produced basaltic amphiboles. *Eur J Miner* 19:641–655
50
51
52
53
54 Al'meev RR, Ariskin AA, Ozerov AYu, Kononkova NN (2002) Problems of the Stoichiometry and
55
56 Thermobarometry of Magmatic Amphiboles: An Example of Hornblende from the Andesites of
57
58 Nezymyannyi Volcano, Eastern Kamchatka. *Geochem Intern* 40:723-738
59
60
61
62
63
64
65

1
2
3
4 Bonadiman C, Nazzareni S, Coltorti M, Comodi P, Giuli G, Faccini B (2014) Crystal chemistry of
5
6 amphiboles: implications for oxygen fugacity and water activity in lithospheric mantle beneath
7
8 Victoria Land, Antarctica. *Contrib Mineral Petrol* 167: 984, DOI 10.1007/s00410-014-0984-8
9
10
11
12 Bottazzi P, Tiepolo M, Vannucci R, Zanetti A, Brumm R, Foley SF, Oberti R (1999) Distinct site
13
14 preferences for heavy and light REE in amphibole and the prediction of $A_{\text{Amph/L}}D_{\text{REE}}$. *Contrib*
15
16 *Mineral Petrol* 137:36-45
17
18
19
20 Cipriani C (2007) Amphiboles: Historical Perspective. *Rev Mineral Geochem* 67:517-546
21
22
23
24 Della Ventura G, Bellatreccia F, Cámara F, Oberti R. (2014) Crystal-chemistry and short-range order
25
26 of fluoro-edenite and fluoro-pargasite: a combined X-ray diffraction and FTIR spectroscopic
27
28 approach. *Miner Mag* 78:293-310
29
30
31
32 Della Ventura G, Susta U, Bellatreccia F, Marcelli A, Redhammer GJ, Oberti R (2017) Deprotonation
33
34 of Fe-dominant amphiboles: Single-crystal HT-FTIR spectroscopic studies of synthetic potassic-
35
36 ferro-richterite. *Am Miner* 102:117-125
37
38
39
40 Dyar MD, Mackwell SJ, McGuire AV, Cross LR, Robertson JD (1993) Crystal chemistry of Fe³⁺ and
41
42 H⁺ in mantle kaersutite: Implications for mantle metasomatism. *Am Miner* 78:968-979
43
44
45
46 Foley S, Tiepolo M, Vannucci R (2002) Growth of early continental crust controlled by melting of
47
48 amphibolite in subduction zones. *Nature* 417:837-840
49
50
51
52 Forbes WC, Starmer RJ (1974) Kaersutite is a possible source of alkali olivine basalts. *Nature* 250:209-
53
54 210
55
56
57
58
59
60
61
62
63
64
65

- 1
2
3
4 Gatta GD, McIntyre GJ, Oberti R, Hawthorne FC (2017) Order of $^{[6]}\text{Ti}^{4+}$ in a Ti- rich calcium
5
6 amphibole from Kaersut, Greenland: a combined X- ray and neutron diffraction study. Phys
7
8 Chem Miner 44:83-94
9
- 10
11
12 Gentili S, Bonadiman C, Biagioni C, Comodi P, Coltorti M, Zucchini A, Ottolini L (2015) Oxo-
13
14 amphiboles in mantle xenoliths: evidence for H₂O-rich melt interacting with the lithospheric
15
16 mantle of Harrow Peaks (Northern Victoria Land, Antarctica). Miner Petrol 109:741-759
17
18
19
- 20
21 Gunter ME, Belluso E, Mottana A (2007) Amphiboles: Environmental and health concerns. Rev Miner
22
23 Geochem 67:453-516
24
25
- 26
27 Hawthorne FC, Ungaretti L, Oberti R, Bottazzi P, Czamanske GK (1993) Li: An important component
28
29 in igneous alkali amphiboles. Am Miner 78:733-745
30
31
- 32
33 Hawthorne FC, Oberti R, Cannillo E, Sardone N, Zanetti A, Grice JD, Ashley PM (1995). A new
34
35 anhydrous amphibole from the Hoskins mine, Grenfell, New South Wales, Australia:
36
37 Description and crystal structure of ungarettiite, $\text{NaNa}_2(\text{Mn}_2^{2+}\text{Mn}_3^{3+})\text{Si}_8\text{O}_{22}\text{O}_2$. Am Miner
38
39 80:165-172
40
41
- 42
43 Hawthorne FC, Oberti R, Della Ventura G, Mottana A (2007) Amphiboles: Crystal Chemistry,
44
45 Occurrence, and Health Issues. Rev Miner Geochem 67: 545 pp
46
47
- 48
49 Hawthorne FC, Oberti R, Harlow GE, Maresch WV, Martin RF, Schumacher JC, Welch MD (2012)
50
51 IMA report Nomenclature of the amphibole supergroup. Am Miner 97:2031-2048
52
53
- 54
55 Hawthorne FC, Oberti R, Cannillo E, Ottolini L, Roelofsen JN, Martin RF (2001) Li-bearing
56
57 arfvedsonitic amphiboles from the Strange Lake peralkaline granite, Quebec. Can Miner
58
59 39:1161-1170
60
61

1
2
3
4 Holland TJB, Blundy JD (1994) Non-ideal interactions in calcic amphiboles and their bearing on
5
6 amphibole-plagioclase thermometry. *Contrib Mineral Petrol* 116:433-447
7
8
9
10 Jackson CRM, Parman SW, Kelley SP, Cooper RF (2013) Noble gas transport into the mantle
11
12 facilitated by high solubility in amphibole. *Nature Geosci* 6:562-565
13
14
15 King PL, Hervig RL, Holloway JR, Vennemann TW, Righter K (1999) Oxy-substitution and
16
17 dehydrogenation in mantle-derived amphibole megacrysts. *Geochim Cosmochim Acta* 63:3635-
18
19 3651
20
21
22
23 King PL, Hervig RL, Holloway JR, Delaney JS, Dyar MD (2000) Partitioning of Fe^{3+}/Fe_{total} between
24
25 amphibole and basanitic melt as a function of oxygen fugacity. *Earth Plan Sci Lett* 178:97-112
26
27
28
29 Langmuir CH, Vocke RD Jr, Hanson GN (1978) A general mixing equation with applications to
30
31 Icelandic basalts. *Earth Planet Sci Lett* 37:380-392
32
33
34
35 Leake BE, Woolley AR, Arps CES, Birch WD, Gilbert MC, Grice JD, Hawthorne FC, Kato A, Kisch
36
37 HJ, Krivovichev VG, Linthout K, Laird J, Mandarino J, Maresch WV, Nickel EH, Schumaker
38
39 JC, Smith DC, Stephenson NCN, Ungaretti L, Whittaker EJW, Youzhi G (1997) Nomenclature
40
41 of amphiboles: report of the subcommittee on amphiboles of the International Mineralogical
42
43 Association Commission on New Minerals and Mineral Names. *Miner Mag* 61:295-321
44
45
46
47
48 Locock AJ (2014) An Excel spreadsheet to classify chemical analyses of amphiboles following the
49
50 IMA2012 recommendations. *Comp Geosci* 62:1–11
51
52
53
54 McCanta MC, Treiman AH, Dyar MD, Alexander CMO'D, Rumble III D, Essene EJ (2008) The LaPaz
55
56 Icefield 04840 meteorite: Mineralogy, metamorphism, and origin of an amphibole-and biotite-
57
58 bearing R chondrite. *Geochim Cosmochim Acta* 72:5757-5780
59
60
61
62
63
64
65

- 1
2
3
4 Oberti R, Ungaretti L, Cannillo E, Hawthorne FC, Memmi I (1995) Temperature-dependent Al order-
5
6 disorder in the tetrahedral double chain of C2/m amphiboles. *Eur J Miner* 7:1049-1063
7
8
9
10 Oberti R, Vannucci R, Zanetti A, Tiepolo M, Brumm RC (2000) A crystal chemical re-evaluation of
11
12 amphibole/melt and amphibole/clinopyroxene D_{Ti} values in petrogenetic studies. *Am Miner*
13
14 85:407-419
15
16
17
18 Oberti R, Cámara F, Ottolini L, Caballero JM (2003) Lithium in amphiboles: detection, quantification,
19
20 and incorporation mechanisms in the compositional space bridging sodic and ^BLi -amphiboles.
21
22 *Eur J Miner* 15:309-319
23
24
25
26 Oberti R, Hawthorne FC, Cannillo E, Cámara F. (2007a) Long-range order in amphiboles. *Rev Miner*
27
28 *Geochem* 67:125-171
29
30
31
32 Oberti R, Boiocchi M, Smith DC, Medenbach O (2007b) Aluminotaramite, alumino-magnesiotalamite,
33
34 and fluoro-alumino-magnesiotalamite: Mineral data and crystal chemistry. *Am Mineral* 92:1428-
35
36 1435.
37
38
39
40 Oberti R, Boiocchi M, Hawthorne FC, Robinson P (2010) Crystal structure and crystal chemistry of
41
42 fluoro-potassic-magnesian-arfvedsonite from Monte Metocha, Xixano region, Mozambique, and
43
44 discussion of the holotype from Quebec, Canada. *Miner Mag* 74:951-960
45
46
47
48 Oberti R, Boiocchi M, Hawthorne FC, Cámara F, Ciriotti ME, Berge SA (2015) Ti-rich Fluoro-
49
50 Richterite from Kariåsen (Norway): the oxo-component and the use of Ti^{4+} as a proxy. *Can*
51
52 *Miner* 53:285-294
53
54
55
56
57
58
59
60
61
62
63
64
65

- 1
2
3
4 Oberti R, Boiocchi M, Hawthorne FC, Ball NA, Cámara F, Pagano R, Pagano A (2016) Ferro-ferri-
5
6 hornblende from the Traversella Mine (Ivrea, Italy): occurrence, mineral description and crystal-
7
8 chemistry. *Miner Mag* 80:1233-1242
9
10
11
12 Oberti R, Boiocchi M, Hawthorne FC, Ball NA, Blass G (2017) Ferri-obertiite from the Rothenberg
13
14 quarry, Eifel volcanic complex, Germany: mineral data and crystal chemistry of a new
15
16 amphibole end-member. *Miner Mag*, doi.org/10.1180/minmag.2016.080.117
17
18
19
20 Ottolini L, Bottazzi P, Zanetti A, Vannucci R (1995) Determination of hydrogen in silicates by Second
21
22 Ion Mass Spectr Anal 120:1309-1314
23
24
25
26 Namur O, Charlier B, Toplis MJ, Auwera JV (2012) Prediction of plagioclase-melt equilibria in
27
28 anhydrous silicate melts at 1 atm. *Contrib Mineral Petrol* 163:133-150
29
30
31
32 Perinelli C, Andreozzi GB, Conte AM, Oberti R, Armienti P (2012) Redox state of subcontinental
33
34 lithospheric mantle and relationships with metasomatism: insights from spinel peridotites from
35
36 northern Victoria Land (Antarctica). *Contrib Mineral Petrol* 164:1053-1067
37
38
39
40 Popp RK, Hibbert HA, Lamb WM (2006) Oxy-amphibole equilibria in Ti-bearing calcic amphiboles:
41
42 Experimental investigation and petrologic implications for mantle-derived amphiboles. *Am*
43
44 *Miner* 91:54-66
45
46
47
48 Ridolfi F, Renzulli A, Puerini M (2010) Stability and chemical equilibrium of amphibole in calc-
49
50 alkaline magmas: an overview, new thermobarometric formulations and application to
51
52 subduction-related volcanoes. *Contrib Mineral Petrol* 160:45-66
53
54
55
56
57
58
59
60
61
62
63
64
65

- 1
2
3
4 Ridolfi F, Renzulli A. (2012) Calcic amphiboles in calc-alkaline and alkaline magmas:
5
6 thermobarometric and chemometric empirical equations valid up to 1,130°C and 2.2 GPa.
7
8 Contrib Mineral Petrol 163:877-895
9
- 10
11
12 Ridolfi F, Renzulli A, Acosta-Vigil A (2014) On the stability of magmatic cordierite and new
13
14 thermobarometric equations for cordierite-saturated liquids. Contrib Mineral Petrol 167:996, doi
15
16 10.1007/s00410-014-0996-4.
17
18
19
- 20
21 Ridolfi F, Braga R, Cesare B, Renzulli A, Perugini D, Del Moro S (2016) Unravelling the complex
22
23 interaction between mantle and crustal magmas encoded in the lavas of San Vincenzo (Tuscany,
24
25 Italy). Part I: Petrography and Thermobarometry. Lithos 244:218-232
26
27
- 28
29 Robinson GW, Grief JD, Gault RA, Lalonde AE (1997) Potassic pargasite, a new member of the
30
31 amphibole group from Pargas, Turku-Pori, Finland. Can Miner 35:1535-1540
32
33
- 34
35 Satoh H, Ymaguchi Y, Makino K (2004) Ti-substitution mechanism in plutonic oxy-kaersutite from the
36
37 Larvik alkaline complex, Oslo rift, Norway. Miner Mag 68:687–697
38
39
- 40
41 Smith DJ (2014) Clinopyroxene precursors to amphibole sponge in arc crust. Nature Comm 5:4329,
42
43 doi:10.1038/ncomms5329.
44
45
- 46
47 Susta U (2016) Dehydration and deprotonation processes in minerals: development of new
48
49 spectroscopic techniques. Unpublished PhD Thesis, University of Roma Tre.
50
- 51
52 Tiepolo M, Vannucci R, Oberti R, Foley S, Bottazzi P, Zanetti A (2000) Nb and Ta incorporation and
53
54 fractionation in titanian pargasite and kaersutite: crystal-chemical constraints and implications for
55
56 natural systems. Earth Planet Sci Lett 176:185-201
57
58
59
60
61
62
63
64
65

- 1
2
3
4 Tiepolo M, Bottazzi P, Foley SF, Oberti R, Vannucci R, Zanetti A (2001) Fractionation of Nb and Ta
5
6 from Zr and Hf at Mantle Depths: the Role of Titanian Pargasite and Kaersutite. *J Petrol* 42:221-
7
8 232
9
10
11
12 Tiepolo M, Zanetti A, Oberti R, Brumm R, Foley S, Vannucci R (2003) Trace-element partitioning
13
14 between synthetic potassic-richterites and silicate melts, and contrasts with the partitioning
15
16 behaviour of pargasites and kaersutites. *Eur J Miner* 15:329-340
17
18
19
20 Ungaretti L (1980) Recent developments in X-ray single crystal diffractometry applied to the crystal-
21
22 chemical study of amphiboles. *Godisn Jugoslav Centra Kristalogr* 15: 29-65
23
24
25
26 Ungaretti L, Smith DC, Rossi G (1981) Crystal-chemistry by X-ray structure refinement and electron
27
28 microprobe analysis of a series of sodic-calcic to alkali amphiboles from the NybO eclogite pod,
29
30 Norway. *Bull Minéral* 104: 400-412
31
32
33
34 Uvarova Y, Sokolova E, Hawthorne FC, McCammon CA, Kazansky VI, Lobanov KV (2007)
35
36 Amphiboles from the Kola Superdeep Borehole: Fe³⁺ contents from crystal-chemical analysis
37
38 and Mössbauer spectroscopy. *Miner Mag* 71:651-669
39
40
41
42 Vannucci R, Piccardo GB, Rivalenti G, Zanetti A, Rampone E, Ottolini L, Oberti R, Mazzucchelli M,
43
44 Bottazzi P (1995) Origin of LREE-depleted amphiboles in the subcontinental mantle. *Geochim*
45
46 *Cosmochim Acta* 59:1763-1771
47
48
49
50
51 Zhang J, Humphreys MCS, Cooper GF, Davidson JP, Macpherson CG (2017) Magma mush chemistry
52
53 at subduction zones, revealed by new melt major element inversion from calcic amphiboles. *Am*
54
55 *Miner*, DOI: <http://dx.doi.org/10.2138/am-2017-5928>
56
57
58
59
60
61
62
63
64
65

1
2
3
4
5
6
7
8
9
10
11
12
13
14
15
16
17
18
19
20
21
22
23
24
25
26
27
28
29
30
31
32
33
34
35
36
37
38
39
40
41
42
43
44
45
46
47
48
49
50
51
52
53
54
55
56
57
58
59
60
61
62
63
64
65

Table captions

Table 1.

Formula and ideal composition (wt%) of the selected Li- and Mn-free monoclinic amphibole end-members and the oxo counterparts for the Ca amphiboles considered in this work. The end-embers are ordered by increasing *Mr*. Values of *cmpg* are also reported for comparison.

Table 2.

Statistic errors of the AMFORM procedure calculated for the compositions used for calibration and for those used in the test. See AMFORM for references and data.

Figure captions

Figure 1.

Plots of CR vs. (a) *Mr*, molecular mass, and (b) *cmpg*, cation mass per gram. The equations (and their statistic values) obtained using normalized and end-member (Table 1) compositions are also reported. Because of EMP analytical errors, the original amphibole compositions show total element oxides varying from 98.3 to 100.8 wt%. Underestimated (< 100 wt%) and overestimated (> 100 wt%) compositions are located above and below the ideal relations, respectively. See the text for further detail.

Figure 2.

(a) Correlation between the measured (reference) ${}^w\text{O}^{2-}$ values and those calculated with equation 3 for 87 amphiboles with ${}^w\text{O}^{2-} \leq 2^{\text{C}}\text{Ti}$ (i.e. poorly-oxidized amphiboles); the 1:1 line is reported together with the standard (σ_{est}) and maximum (Max) errors. (b) best correlation found between the reference

1
2
3
4 $^w\text{O}^{2-}$ values and cation composition for all the 114 high-quality amphibole compositions. The red
5
6 broken lines describe the proposed relation; related equations and statistic errors are also reported in
7
8 red. See text for further detail.
9

10
11
12 Figure 3.

13
14
15 The correlation between *TC* (totals coefficient) values and those calculated with equation 5 for the 342
16 corrected compositions (either normalized or deviated) and the 114 original compositions. Wt% in bold
17 indicate the normalized and deviated total element oxides; maximum and minimum uncertainties are
18
19 +0.005 and -0.004.
20
21
22
23
24
25

26 Figure 4.

27
28
29 The correlation between the reference ^TSi (a), ^CAl (b), ^BNa (c) and $^A(\text{Ca} + \text{Na} + \text{K})$ (d) values and those
30 calculated with the AMFORM spreadsheet for the amphibole compositions used to calibrate the
31 procedure (blue diamonds) and for those used for testing (yellow triangles). The 1:1 lines are reported
32
33 in all diagrams (see Table 2 for statistics).
34
35
36
37
38
39

40 Figure 5.

41
42
43 The correlation between the reference ^CAl , $^A(\text{Ca} + \text{Na} + \text{K})$ and $^C\text{Fe}^{3+}$ values (from EMP+SREF±SIMS
44 data) and those solely calculated from the high-quality EMP analysis in our dataset; (a-c): AMFORM;
45
46 (d-f): Locock (2014) without $^w\text{O}^{2-}$ estimates; (g-i): Locock (2014) with $^w\text{O}^{2-}$ estimates. Symbols as in
47
48 Fig. 2a. The statistics in diagrams (c), (f), (i) for Fe^{3+} refer to the 87 amphiboles with $^w\text{O}^{2-} \leq 2^C\text{Ti}$,
49
50 whereas those in diagrams (a), (d), (g) for ^CAl and (b), (e), (h) for $^A(\text{Ca} + \text{Na} + \text{K})$ refer to all the 114
51 amphiboles in the dataset; max and min errors are the maximum and minimum (calculated – reference)
52
53 values. The orange empty squares in (c), (f), (i) represent highly-oxidized amphiboles with $^w\text{O}^{2-} >$
54
55 2^CTi ; diagram (c) also includes some amphiboles taken from the literature with $^w\text{O}^{2-} \leq 2^C\text{Ti}$, the
56
57
58
59
60
61
62
63
64
65

1
2
3
4 $\text{Fe}^{3+}/\text{Fe}_{\text{tot}}$ value of which was measured using independent techniques (yellow squares; King et al.
5
6
7 2000; Satoh et al. 2004; Bonadiman et al. 2014). The 1:1 line is reported in all diagrams.
8
9

10 Figure 6.

11
12
13 Correlations between the reference $^{\text{W}}\text{O}^{2-}$ and Fe^{3+} values and those calculated with the default (a-b) and
14
15 the optional (c-d) procedures in AMFORM for the 114 compositions used for calibration and the 13
16
17 compositions with Fe^{3+} measured by independent techniques. In (a) and (b), statistics refer only to
18
19 highly-oxidized Ca amphiboles (with $^{\text{W}}\text{O}^{2-} > ^{\text{C}}\text{Ti}$) and ferri-kaersutites (symbols have the same color of
20
21 statistic values); see Fig. 2a and 4c for symbols and the statistics of poorly-oxidized amphiboles. In (c)
22
23 and (d) statistics refer to all the 127 amphiboles considered.
24
25
26
27
28
29
30
31
32
33
34
35
36
37
38
39
40
41
42
43
44
45
46
47
48
49
50
51
52
53
54
55
56
57
58
59
60
61
62
63
64
65

Fig 1.

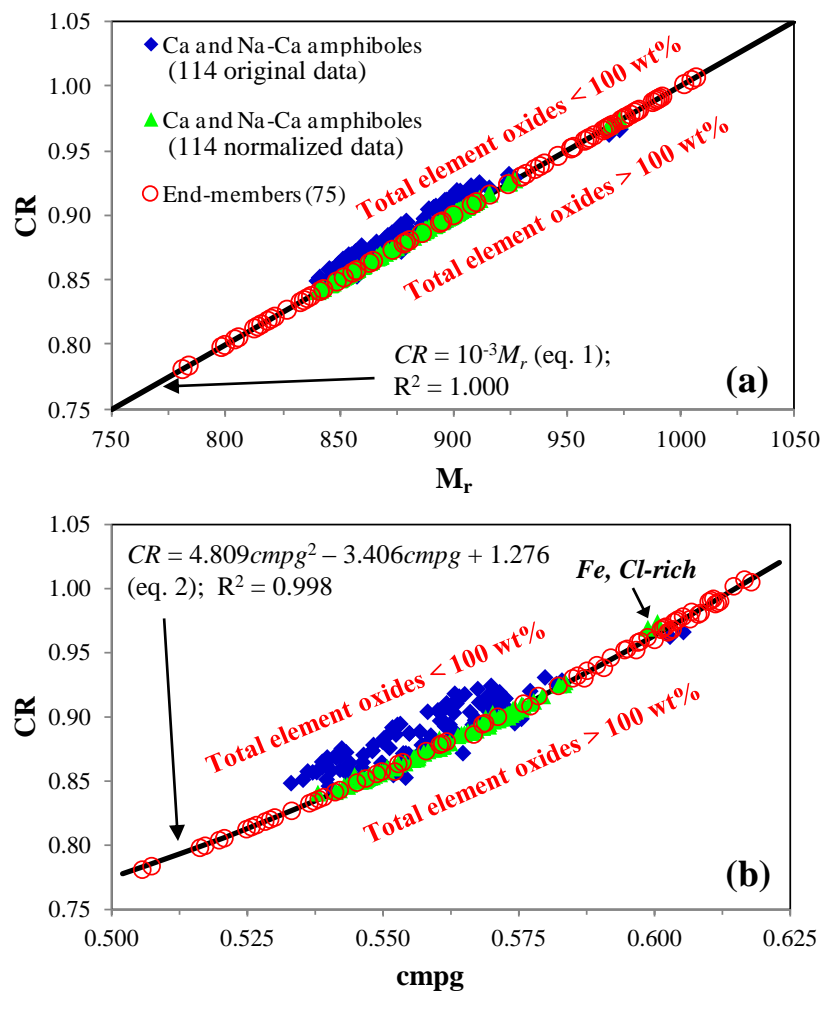


Fig 2.

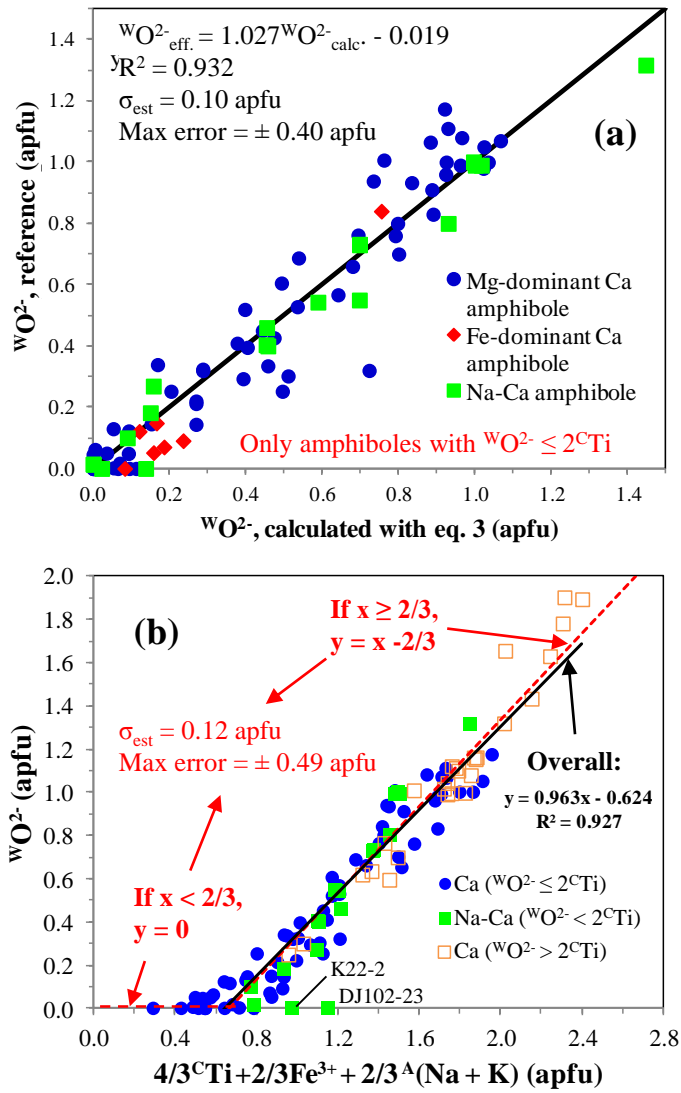


Fig 3.

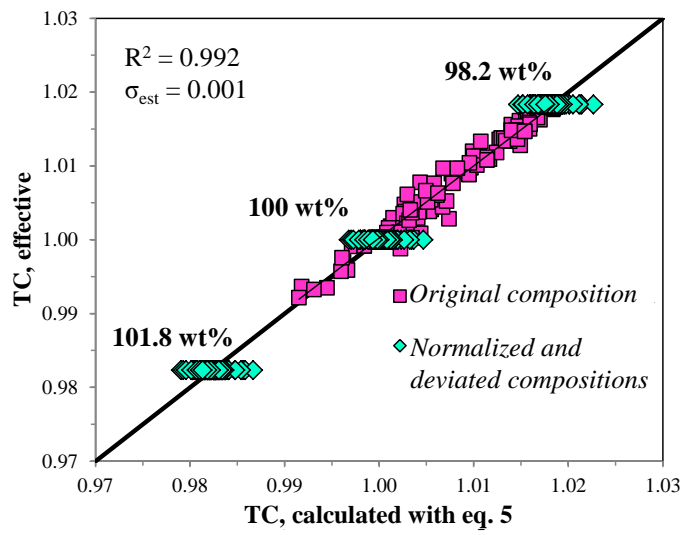


Fig 4.

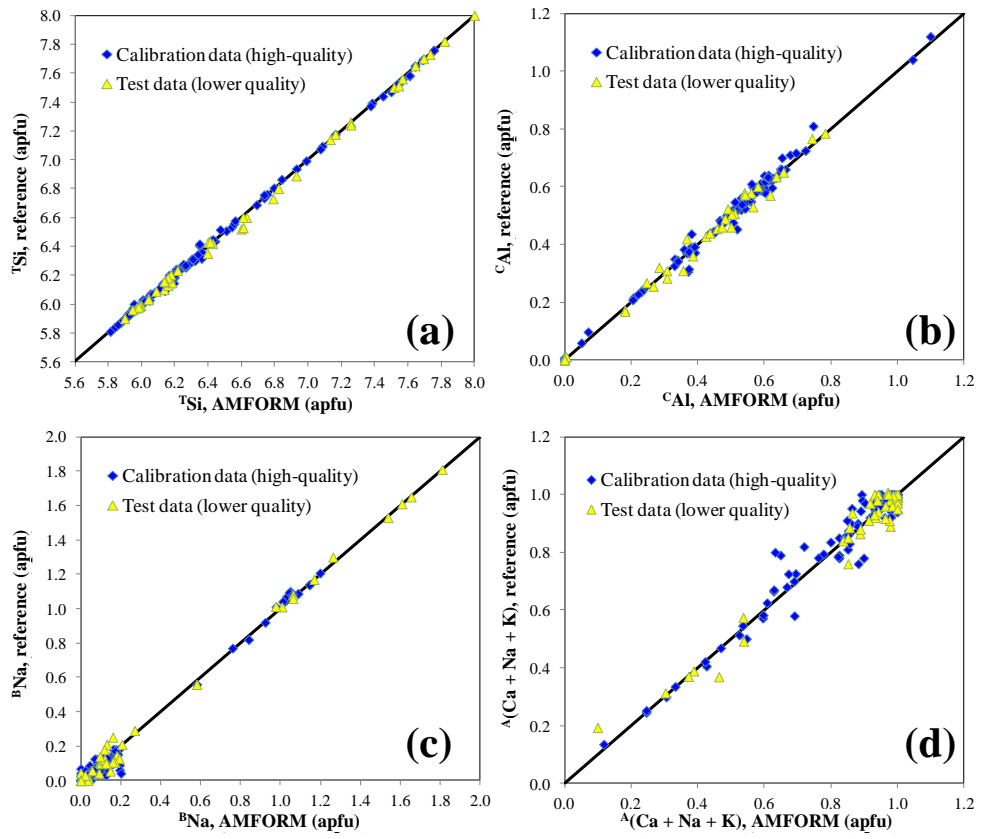


Fig 5.

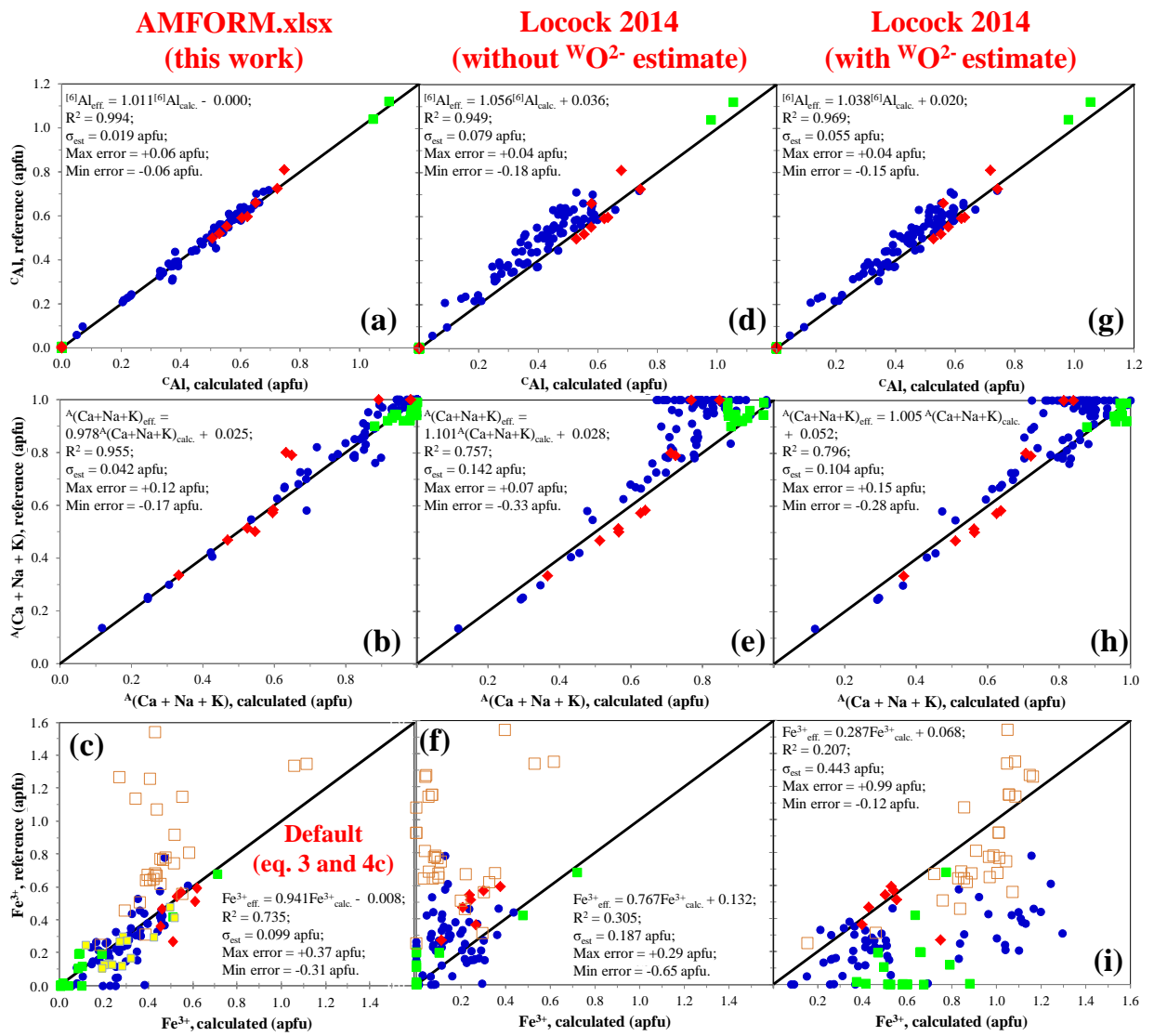


Fig 6.

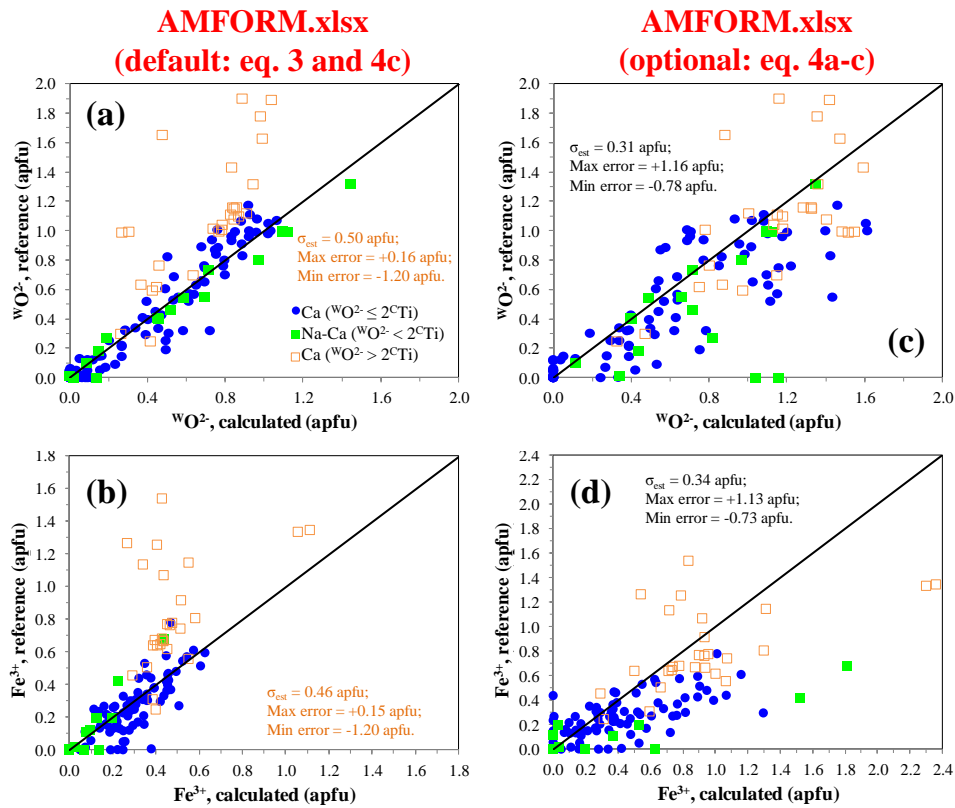


Table 1.

Name	Group	Sub-group	Formula	SiO ₂	TiO ₂	Al ₂ O ₃	FeO _{tot}	MgO	CaO	Na ₂ O	Sum	Fe ₂ O ₃	FeO	H ₂ O	M _r	cmpg
Cumingtonite	^W (OH,F,Cl)	Mg-Fe-Mn	□Mg ₂ Mg ₅ Si ₈ O ₂₂ (OH) ₂	61.56	0.00	0.00	0.00	36.13	0.00	0.00	97.69			2.31	781	0.506
Glaucofanite	^W (OH,F,Cl)	Na	□Na ₂ (Mg ₃ Al ₂)Si ₈ O ₂₂ (OH) ₂	61.35	0.00	13.01	0.00	15.43	0.00	7.91	97.70			2.30	784	0.507
Winchite	^W (OH,F,Cl)	Na-Ca	□(NaCa)(Mg ₄ Al)Si ₈ O ₂₂ (OH) ₂	60.24	0.00	6.39	0.00	20.20	7.03	3.88	97.74			2.26	798	0.516
Barroisite	^W (OH,F,Cl)	Na-Ca	□(NaCa)(Mg ₃ Al ₂)(Si ₇ Al)O ₂₂ (OH) ₂	52.60	0.00	19.13	0.00	15.12	7.01	3.88	97.75			2.25	800	0.517
Eckermannite	^W (OH,F,Cl)	Na	NaNa ₂ (Mg ₄ Al)Si ₈ O ₂₂ (OH) ₂	59.80	0.00	6.34	0.00	20.06	0.00	11.57	97.76			2.24	804	0.520
Nyboite	^W (OH,F,Cl)	Na	NaNa ₂ (Mg ₃ Al ₂)(Si ₇ Al)O ₂₂ (OH) ₂	52.22	0.00	18.99	0.00	15.01	0.00	11.54	97.76			2.24	805	0.521
Tremolite	^W (OH,F,Cl)	Ca	□Ca ₂ Mg ₅ Si ₈ O ₂₂ (OH) ₂	59.17	0.00	0.00	0.00	24.81	13.81	0.00	97.78			2.22	812	0.525
Magnesio-hornblende	^W (OH,F,Cl)	Ca	□Ca ₂ (Mg ₄ Al)(Si ₇ Al)O ₂₂ (OH) ₂	51.67	0.00	12.53	0.00	19.81	13.78	0.00	97.79			2.21	814	0.526
Tschermakite	^W (OH,F,Cl)	Ca	□Ca ₂ (Mg ₃ Al ₂)(Si ₆ Al ₂)O ₂₂ (OH) ₂	44.21	0.00	25.01	0.00	14.83	13.75	0.00	97.79			2.21	815	0.527
Richterite	^W (OH,F,Cl)	Na-Ca	Na(NaCa)Mg ₅ Si ₈ O ₂₂ (OH) ₂	58.74	0.00	0.00	0.00	24.63	6.85	7.57	97.80			2.20	818	0.528
Katophorite	^W (OH,F,Cl)	Na-Ca	Na(NaCa)(Mg ₄ Al)(Si ₇ Al)O ₂₂ (OH) ₂	51.30	0.00	12.44	0.00	19.66	6.84	7.56	97.80			2.20	820	0.529
Taramite	^W (OH,F,Cl)	Na-Ca	Na(NaCa)(Mg ₃ Al ₂)(Si ₆ Al ₂)O ₂₂ (OH) ₂	43.89	0.00	24.83	0.00	14.72	6.83	7.55	97.81			2.19	821	0.530
Ferri-winchite	^W (OH,F,Cl)	Na-Ca	□(NaCa)(Mg ₄ Fe ³⁺)Si ₈ O ₂₂ (OH) ₂	58.14	0.00	0.00	8.69	19.50	6.78	3.75	96.85	9.66	0.00	2.18	827	0.533
Magnesio-arfvedsonite	^W (OH,F,Cl)	Na	NaNa ₂ (Mg ₄ Fe ³⁺)Si ₈ O ₂₂ (OH) ₂	57.72	0.00	0.00	8.63	19.36	0.00	11.16	96.88	9.59	0.00	2.16	833	0.536
Edenite	^W (OH,F,Cl)	Ca	NaCa ₂ Mg ₅ (Si ₇ Al)O ₂₂ (OH) ₂	50.41	0.00	6.11	0.00	24.16	13.44	3.71	97.84			2.16	834	0.537
Pargasite	^W (OH,F,Cl)	Ca	NaCa ₂ (Mg ₄ Al)(Si ₆ Al ₂)O ₂₂ (OH) ₂	43.13	0.00	18.30	0.00	19.29	13.42	3.71	97.84			2.16	836	0.538
Sadanagaite	^W (OH,F,Cl)	Ca	NaCa ₂ (Mg ₃ Al ₂)(Si ₅ Al ₃)O ₂₂ (OH) ₂	35.88	0.00	30.44	0.00	14.44	13.39	3.70	97.85			2.15	837	0.539
Magnesio-riebeckite	^W (OH,F,Cl)	Na	□Na ₂ (Mg ₃ Fe ³⁺)Si ₈ O ₂₂ (OH) ₂	57.14	0.00	0.00	17.08	14.37	0.00	7.37	95.96	18.98	0.00	2.14	841	0.541
Magnesio-ferri-hornblende	^W (OH,F,Cl)	Ca	□Ca ₂ (Mg ₄ Fe ³⁺)(Si ₇ Al)O ₂₂ (OH) ₂	49.90	0.00	6.05	8.52	19.13	13.31	0.00	96.91	9.47	0.00	2.14	843	0.542
Ferri-katophorite	^W (OH,F,Cl)	Na-Ca	Na(NaCa)(Mg ₄ Fe ³⁺)(Si ₇ Al)O ₂₂ (OH) ₂	49.56	0.00	6.01	8.47	19.00	6.61	7.30	96.93	9.41	0.00	2.12	849	0.545
Cannilloite	^W (OH,F,Cl)	Ca	CaCa ₂ (Mg ₄ Al)(Si ₅ Al ₃)O ₂₂ (OH) ₂	35.27	0.00	23.94	0.00	18.93	19.75	0.00	97.89			2.11	852	0.547
Rootname 4	^W (OH,F,Cl)	Ca	NaCa ₂ (Mg ₄ Ti)(Si ₅ Al ₃)O ₂₂ (OH) ₂	35.11	9.33	17.88	0.00	18.84	13.11	3.62	97.89			2.11	856	0.549
Kaersutite	^W O	-	NaCa ₂ (Mg ₃ TiAl)(Si ₆ Al ₂)O ₂₂ O ₂	42.05	9.32	17.84	0.00	14.10	13.08	3.61	100.00			0.00	857	0.552
Ferri-barroisite	^W (OH,F,Cl)	Na-Ca	Na(NaCa)(Mg ₃ Fe ³⁺)(Si ₇ Al)O ₂₂ (OH) ₂	49.06	0.00	5.95	16.76	14.10	6.54	3.61	96.03	18.63	0.00	2.10	857	0.550
Ferri-nyboite	^W (OH,F,Cl)	Na	NaNa ₂ (Mg ₃ Fe ³⁺)(Si ₇ Al)O ₂₂ (OH) ₂	48.73	0.00	5.91	16.65	14.01	0.00	10.77	96.06	18.50	0.00	2.09	863	0.553
Magnesio-hastingsite	^W (OH,F,Cl)	Ca	NaCa ₂ (Mg ₄ Fe ³⁺)(Si ₆ Al ₂)O ₂₂ (OH) ₂	41.69	0.00	11.79	8.31	18.64	12.97	3.58	96.99	9.23	0.00	2.08	865	0.554
Ferri-tschermakite	^W (OH,F,Cl)	Ca	□Ca ₂ (Mg ₃ Fe ³⁺)(Si ₆ Al ₂)O ₂₂ (OH) ₂	41.28	0.00	11.68	16.45	13.85	12.84	0.00	96.10	18.29	0.00	2.06	873	0.558
Ferro-glaucofanite	^W (OH,F,Cl)	Na	□Na ₂ (Fe ²⁺ ₃ Al ₂)Si ₈ O ₂₂ (OH) ₂	54.74	0.00	11.61	24.54	0.00	0.00	7.06	97.95	0.00	24.54	2.05	878	0.560
Ferri-taramite	^W (OH,F,Cl)	Na-Ca	Na(NaCa)(Mg ₃ Fe ³⁺)(Si ₆ Al ₂)O ₂₂ (OH) ₂	41.01	0.00	11.60	16.34	13.75	6.38	7.05	96.13	18.16	0.00	2.05	879	0.561
Ferri-cannilloite	^W (OH,F,Cl)	Ca	CaCa ₂ (Mg ₄ Fe ³⁺)(Si ₅ Al ₃)O ₂₂ (OH) ₂	34.11	0.00	17.37	8.16	18.31	19.10	0.00	97.05	9.07	0.00	2.05	881	0.562
Ferri-kaersutite	^W O	-	NaCa ₂ (Mg ₃ TiFe ³⁺)(Si ₆ Al ₂)O ₂₂ O ₂	40.68	9.01	11.51	8.11	13.64	12.66	3.50	99.10	9.01	0.00	0.00	886	0.567
Ferro-barroisite	^W (OH,F,Cl)	Na-Ca	□(NaCa)(Fe ²⁺ ₃ Al ₂)(Si ₇ Al)O ₂₂ (OH) ₂	47.04	0.00	17.10	24.11	0.00	6.27	3.47	97.99	0.00	24.11	2.01	894	0.568
Ferri-sadanagaite	^W (OH,F,Cl)	Ca	NaCa ₂ (Mg ₃ Fe ³⁺)(Si ₅ Al ₃)O ₂₂ (OH) ₂	33.56	0.00	17.09	16.05	13.51	12.53	3.46	96.20	17.84	0.00	2.01	895	0.569
Ferro-nyboite	^W (OH,F,Cl)	Na	NaNa ₂ (Fe ²⁺ ₃ Al ₂)(Si ₇ Al)O ₂₂ (OH) ₂	46.73	0.00	16.99	23.95	0.00	0.00	10.33	98.00	0.00	23.95	2.00	900	0.571
oxo Ferro-tschermakite	^W O	Ca	□Ca ₂ (Fe ²⁺ ₂ Fe ³⁺ ₂ Al ₂)(Si ₆ Al ₂)O ₂₂ O ₂	39.70	0.00	22.46	23.73	0.00	12.35	0.00	98.24	17.58	7.91	0.00	908	0.577
Ferro-tschermakite	^W (OH,F,Cl)	Ca	□Ca ₂ (Fe ²⁺ ₃ Al ₂)(Si ₆ Al ₂)O ₂₂ (OH) ₂	39.61	0.00	22.41	23.68	0.00	12.32	0.00	98.02	0.00	23.68	1.98	910	0.576
Ferro-taramite	^W (OH,F,Cl)	Na-Ca	Na(NaCa)(Fe ²⁺ ₃ Al ₂)(Si ₆ Al ₂)O ₂₂ (OH) ₂	39.35	0.00	22.26	23.53	0.00	6.12	6.77	98.03	0.00	23.53	1.97	916	0.579
Ferro-winchite	^W (OH,F,Cl)	Na-Ca	□(NaCa)(Fe ²⁺ ₄ Al)Si ₈ O ₂₂ (OH) ₂	52.01	0.00	5.52	31.10	0.00	6.07	3.35	98.05	0.00	31.10	1.95	924	0.582
oxo Ferro-sadanagaite	^W O	Ca	NaCa ₂ (Fe ²⁺ ₂ Fe ³⁺ ₂ Al ₂)(Si ₅ Al ₃)O ₂₂ O ₂	32.30	0.00	27.41	23.18	0.00	12.06	3.33	98.28	17.17	7.73	0.00	930	0.587
Ferro-eckermannite	^W (OH,F,Cl)	Na	NaNa ₂ (Fe ²⁺ ₄ Al)Si ₈ O ₂₂ (OH) ₂	51.68	0.00	5.48	30.90	0.00	0.00	10.00	98.06	0.00	30.90	1.94	930	0.585
Ferro-sadanagaite	^W (OH,F,Cl)	Ca	NaCa ₂ (Fe ²⁺ ₃ Al ₂)(Si ₅ Al ₃)O ₂₂ (OH) ₂	32.23	0.00	27.35	23.13	0.00	12.03	3.33	98.07	0.00	23.13	1.93	932	0.586
Riebeckite	^W (OH,F,Cl)	Na	□Na ₂ (Fe ²⁺ ₃ Fe ³⁺ ₂)Si ₈ O ₂₂ (OH) ₂	51.36	0.00	0.00	38.38	0.00	0.00	6.62	96.37	17.06	23.03	1.92	936	0.588
oxo Ferro-hornblende	^W O	Ca	□Ca ₂ (Fe ²⁺ ₂ Fe ³⁺ ₂ Al)(Si ₇ Al)O ₂₂ O ₂	44.83	0.00	10.87	30.63	0.00	11.96	0.00	98.29	17.02	15.32	0.00	938	0.591
Ferro-hornblende	^W (OH,F,Cl)	Ca	□Ca ₂ (Fe ²⁺ ₄ Al)(Si ₇ Al)O ₂₂ (OH) ₂	44.74	0.00	10.85	30.57	0.00	11.93	0.00	98.08	0.00	30.57	1.92	940	0.589
Ferro-katophorite	^W (OH,F,Cl)	Na-Ca	Na(NaCa)(Fe ²⁺ ₄ Al)(Si ₇ Al)O ₂₂ (OH) ₂	44.46	0.00	10.78	30.38	0.00	5.93	6.55	98.10	0.00	30.38	1.90	946	0.592
Ferro-ferri-barroisite	^W (OH,F,Cl)	Na-Ca	□(NaCa)(Fe ²⁺ ₃ Fe ³⁺ ₂)(Si ₇ Al)O ₂₂ (OH) ₂	44.19	0.00	5.36	37.74	0.00	5.89	3.26	96.43	16.78	22.64	1.89	952	0.594
Ferro-kaersutite	^W O	-	NaCa ₂ (Fe ²⁺ ₃ TiAl)(Si ₆ Al ₂)O ₂₂ O ₂	37.87	8.39	16.07	22.64	0.00	11.78	3.26	100.00	0.00	22.64	0.00	952	0.597
Ferro-ferri-winchite	^W (OH,F,Cl)	Na-Ca	□(NaCa)(Fe ²⁺ ₄ Fe ³⁺)Si ₈ O ₂₂ (OH) ₂	50.44	0.00	0.00	37.69	0.00	5.88	3.25	97.27	8.38	30.16	1.89	953	0.595
Ferro-ferri-nyboite	^W (OH,F,Cl)	Na	NaNa ₂ (Fe ²⁺ ₃ Fe ³⁺ ₂)(Si ₇ Al)O ₂₂ (OH) ₂	43.91	0.00	5.32	37.51	0.00	0.00	9.71	96.45	16.67	22.50	1.88	958	0.597
Arfvedsonite	^W (OH,F,Cl)	Na	NaNa ₂ (Fe ²⁺ ₄ Fe ³⁺)Si ₈ O ₂₂ (OH) ₂	50.13	0.00	0.00	37.46	0.00	0.00	9.70	97.29	8.33	29.97	1.88	959	0.597
oxo Ferro-pargasite	^W O	Ca	NaCa ₂ (Fe ²⁺ ₂ Fe ³⁺ ₂ Al)(Si ₆ Al ₂)O ₂₂ O ₂	37.55	0.00	15.93	29.94	0.00	11.68	3.23	98.33	16.63	14.97	0.00	960	0.600
Ferro-pargasite	^W (OH,F,Cl)	Ca	NaCa ₂ (Fe ²⁺ ₄ Al)(Si ₆ Al ₂)O ₂₂ (OH) ₂	37.47	0.00	15.90	29.87	0.00	11.66	3.22	98.13	0.00	2			

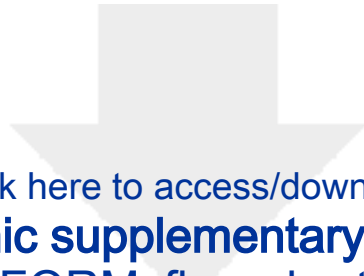
Table 1. Continue.

Name	Group	Sub-group	Formula	SiO ₂	TiO ₂	Al ₂ O ₃	FeO _{tot}	MgO	CaO	Na ₂ O	Sum	Fe ₂ O ₃	FeO	H ₂ O	M _r	cmg
oxo Ferro-ferri-hornblende	^W O	Ca	□Ca ₂ (Fe ²⁺ ₂ Fe ³⁺ ₃)(Si ₇ Al)O ₂₂ O ₂	43.50	0.00	5.27	37.15	0.00	11.60	0.00	97.52	24.77	14.86	0.00	967	0.603
oxo Ferro-cannilloite	^W O	Ca	CaCa ₂ (Fe ²⁺ ₂ Fe ³⁺ ₂ Al)(Si ₅ Al ₃)O ₂₂ O ₂	30.78	0.00	20.89	29.45	0.00	17.24	0.00	98.36	16.36	14.72	0.00	976	0.607
oxo Ferro-ferri-tschermakite	^W O	Ca	□Ca ₂ (Fe ²⁺ ₃ Fe ³⁺ ₄)(Si ₆ Al ₂)O ₂₂ O ₂	37.33	0.00	10.56	37.19	0.00	11.61	0.00	96.69	33.07	7.44	0.00	966	0.602
Ferro-ferri-tschermakite	^W (OH,F,Cl)	Ca	□Ca ₂ (Fe ²⁺ ₃ Fe ³⁺ ₂)(Si ₆ Al ₂)O ₂₂ (OH) ₂	37.25	0.00	10.53	37.12	0.00	11.59	0.00	96.49	16.50	22.27	1.86	968	0.601
oxo Ferro-actinolite	^W O	Ca	□Ca ₂ (Fe ²⁺ ₃ Fe ³⁺ ₂)Si ₈ O ₂₂ O ₂	49.65	0.00	0.00	37.11	0.00	11.59	0.00	98.35	16.50	22.26	0.00	968	0.603
Ferro-ferri-hornblende	^W (OH,F,Cl)	Ca	□Ca ₂ (Fe ²⁺ ₄ Fe ³⁺ ₁)(Si ₇ Al)O ₂₂ (OH) ₂	43.41	0.00	5.26	37.07	0.00	11.57	0.00	97.32	8.24	29.66	1.86	969	0.602
Ferro-actinolite	^W (OH,F,Cl)	Ca	□Ca ₂ Fe ²⁺ ₅ Si ₈ O ₂₂ (OH) ₂	49.55	0.00	0.00	37.03	0.00	11.56	0.00	98.14	0.00	37.03	1.86	970	0.602
Ferro-ferri-taramite	^W (OH,F,Cl)	Na-Ca	Na(NaCa)(Fe ²⁺ ₃ Fe ³⁺ ₂)(Si ₆ Al ₂)O ₂₂ (OH) ₂	37.02	0.00	10.47	36.89	0.00	5.76	6.36	96.51	16.40	22.13	1.85	974	0.604
Ferro-ferri-katophorite	^W (OH,F,Cl)	Na-Ca	Na(NaCa)(Fe ²⁺ ₄ Fe ³⁺ ₁)(Si ₇ Al)O ₂₂ (OH) ₂	43.14	0.00	5.23	36.85	0.00	5.75	6.36	97.33	8.19	29.48	1.85	975	0.604
Ferro-richterite	^W (OH,F,Cl)	Na-Ca	Na(NaCa)Fe ²⁺ ₅ Si ₈ O ₂₂ (OH) ₂	49.25	0.00	0.00	36.81	0.00	5.75	6.35	98.15	0.00	36.81	1.85	976	0.604
Ferro-cannilloite	^W (OH,F,Cl)	Ca	CaCa ₂ (Fe ²⁺ ₄ Al)(Si ₅ Al ₃)O ₂₂ (OH) ₂	30.72	0.00	20.85	29.39	0.00	17.20	0.00	98.16	0.00	29.39	1.84	978	0.605
oxo Ferro-rootname 4	^W O	Ca	NaCa ₂ (Fe ²⁺ ₂ Fe ³⁺ ₂ Ti)(Si ₅ Al ₃)O ₂₂ O ₂	30.66	8.15	15.61	29.33	0.00	11.45	3.16	98.37	16.30	14.67	0.00	980	0.608
Ferro-ferri-kaersutite	^W O	-	NaCa ₂ (Fe ²⁺ ₃ TiFe ³⁺ ₁)(Si ₅ Al ₃)O ₂₂ O ₂	36.75	8.14	10.40	29.30	0.00	11.43	3.16	99.18	8.14	21.97	0.00	981	0.609
Ferro-rootname 4	^W (OH,F,Cl)	Ca	NaCa ₂ (Fe ²⁺ ₄ Ti)(Si ₅ Al ₃)O ₂₂ (OH) ₂	30.60	8.13	15.58	29.27	0.00	11.42	3.16	98.17	0.00	29.27	1.83	982	0.607
oxo Ferro-ferri-sadanagaite	^W O	Ca	NaCa ₂ (Fe ²⁺ ₃ Fe ³⁺ ₄)(Si ₅ Al ₃)O ₂₂ O ₂	30.42	0.00	15.48	36.37	0.00	11.35	3.14	96.76	32.33	7.27	0.00	988	0.611
oxo Hastingsite	^W O	Ca	NaCa ₂ (Fe ²⁺ ₂ Fe ³⁺ ₃)(Si ₆ Al ₂)O ₂₂ O ₂	36.46	0.00	10.31	36.33	0.00	11.34	3.13	97.57	24.22	14.53	0.00	989	0.612
Ferro-ferri-sadanagaite	^W (OH,F,Cl)	Ca	NaCa ₂ (Fe ²⁺ ₃ Fe ³⁺ ₂)(Si ₅ Al ₃)O ₂₂ (OH) ₂	30.35	0.00	15.45	36.29	0.00	11.33	3.13	96.56	16.13	21.78	1.82	990	0.610
oxo Ferro-edenite	^W O	Ca	NaCa ₂ (Fe ²⁺ ₃ Fe ³⁺ ₂)(Si ₇ Al)O ₂₂ O ₂	42.49	0.00	5.15	36.29	0.00	11.33	3.13	98.38	16.13	21.77	0.00	990	0.612
Hastingsite	^W (OH,F,Cl)	Ca	NaCa ₂ (Fe ²⁺ ₄ Fe ³⁺ ₁)(Si ₆ Al ₂)O ₂₂ (OH) ₂	36.38	0.00	10.29	36.25	0.00	11.32	3.13	97.37	8.06	29.00	1.82	991	0.610
Ferro-edenite	^W (OH,F,Cl)	Ca	NaCa ₂ Fe ²⁺ ₅ (Si ₇ Al)O ₂₂ (OH) ₂	42.40	0.00	5.14	36.21	0.00	11.31	3.12	98.18	0.00	36.21	1.82	992	0.611
Grunerite	^W (OH,F,Cl)	Mg-Fe-Mn	□Fe ²⁺ ₂ Fe ²⁺ ₅ Si ₈ O ₂₂ (OH) ₂	47.99	0.00	0.00	50.21	0.00	0.00	0.00	98.20	0.00	50.21	1.80	1002	0.615
oxo Ferro-ferri-cannilloite	^W O	Ca	CaCa ₂ (Fe ²⁺ ₂ Fe ³⁺ ₃)(Si ₅ Al ₃)O ₂₂ O ₂	29.90	0.00	15.22	35.75	0.00	16.74	0.00	97.61	23.84	14.30	0.00	1005	0.618
Ferro-ferri-cannilloite	^W (OH,F,Cl)	Ca	CaCa ₂ (Fe ²⁺ ₄ Fe ³⁺ ₁)(Si ₅ Al ₃)O ₂₂ (OH) ₂	29.84	0.00	15.19	35.68	0.00	16.71	0.00	97.42	7.93	28.54	1.79	1007	0.617

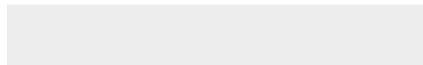
Table 2.

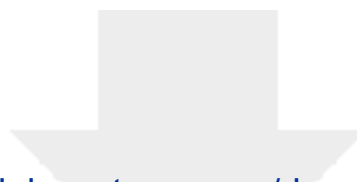
Amphibole parameter	Calibration high-quality data N = 114		Test lower-quality data N = 34	
	σ_{est}	max error	σ_{est}	max error
^T Si	0.017	0.068	0.028	0.081
^C Al	0.019	0.065	0.022	0.052
^C Ti	0.012	0.087	0.008	0.040
Fe _T	0.007	0.045	0.027	0.121
Mg _T	0.008	0.028	0.015	0.045
Ca _T	0.005	0.019	0.005	0.012
^B Na	0.036	0.159	0.036	0.093
^A Na	0.038	0.165	0.038	0.094
^A K	0.002	0.007	0.002	0.005
^A (Ca + Na + K)	0.042	0.168	0.042	0.094
F	0.004	0.016	0.015	0.060
$\Delta\text{MM}\%$	0.18	0.74	0.26	0.87

N: sample number; σ_{est} : error standard of the estimate; max error: maximum error



Click here to access/download
Electronic supplementary material
AMFORM_flow chart.pdf





Click here to access/download

Electronic supplementary material
AMFORM.xlsx

